First Measurement of the Hubble Constant from a Dark Standard Siren using the Dark Energy Survey Galaxies and the LIGO/Virgo Binary–Black-hole Merger GW170814

The Astrophysical Journal Letters, 876:L7 (15pp), 2019 May 1 https://doi.org/10.3847/2041-8213/ab14f1

First Measurement of the Hubble Constant from a Dark Standard Siren using the Dark Energy Survey Galaxies and the LIGO/Virgo Binary–Black-hole Merger GW170814

M. Soares-Santos[1], A. Palmese[2], W. Hartley[3], J. Annis[2], J. Garcia-Bellido[4], O. Lahav[3], Z. Doctor[5,6], M. Fishbach[6], D. E. Holz[7], H. Lin[2], M. E. S. Pereira[1], A. Garcia[1], K. Herner[2], R. Kessler[6,8], H. V. Peiris[3], M. Sako[9], S. Allam[2], D. Brout[9], A. Carnero Rosell[10,11], H. Y. Chen[7], C. Conselice[12], J. deRose[13,14], J. deVicente[10], H. T. Diehl[2], M. S. S. Gill[15], J. Gschwend[11,16], I. Sevilla-Noarbe[10], D. L. Tucker[2], R. Wechsler[15,17,18], E. Berger[19], P. S. Cowperthwaite[20,227], B. D. Metzger[21], P. K. G. Williams[19,22], T. M. C. Abbott[23], F. B. Abdalla[3], S. Avila[24], K. Bechtol[25,26], E. Bertin[27,28], D. Brooks[3], E. Buckley-Geer[2], D. L. Burke[15,18], M. Carrasco Kind[29,30], J. Carretero[31], F. J. Castander[32,33], M. Crocce[33,32], C. E. Cunha[18], C. B. D'Andrea[9], L. N. da Costa[11,16], C. Davis[18], S. Desai[34], P. Doel[3], A. Drlica-Wagner[2,7], T. F. Eifler[35,36], A. E. Evrard[37,38], B. Flaugher[2], P. Fosalba[32,33], J. Frieman[2,6], E. Gaztanaga[32,33], D. W. Gerdes[37,38], D. Gruen[15,18], R. A. Gruendl[29,30], G. Gutierrez[2], D. L. Hollowood[39], B. Hoyle[40,41], D. J. James[42], T. Jeltema[39], K. Kuehn[43], N. Kuropatkin[2], T. S. Li[2,6], M. Lima[11,44], M. A. G. Maia[11,16], J. L. Marshall[45], F. Menanteau[29,30], R. Miquel[31,46], E. Neilsen[2], R. L. C. Ogando[11,16], A. A. Plazas[36,47], A. K. Romer[48], A. Roodman[15,18], E. Sanchez[10], V. Scarpine[2], R. Schindler[15], M. Schubnell[38], S. Serrano[32,33], M. Smith[49], R. C. Smith[23], F. Sobreira[11,50], E. Suchyta[51], M. E. C. Swanson[30], G. Tarle[38], R. C. Thomas[52], A. R. Walker[23], W. Wester[2], J. Zuntz[53]

(The DES Collaboration),

and

B. P. Abbott[54], R. Abbott[54], T. D. Abbott[55], S. Abraham[56], F. Acernese[57,58], K. Ackley[59], C. Adams[60], R. X. Adhikari[54], V. B. Adya[61,62], C. Affeldt[61,62], M. Agathos[63], K. Agatsuma[64], N. Aggarwal[65], O. D. Aguiar[66], L. Aiello[67,68], A. Ain[56], P. Ajith[69], G. Allen[70], A. Allocca[71,72], M. A. Aloy[73], P. A. Altin[74], A. Amato[75], A. Ananyeva[54], S. B. Anderson[54], W. G. Anderson[76], S. V. Angelova[77], S. Appert[54], K. Arai[54], M. C. Araya[54], J. S. Areeda[78], M. Arène[79], S. Ascenzi[80,81], G. Ashton[59], S. M. Aston[60], P. Astone[82], F. Aubin[83], P. Aufmuth[62], K. AultONeal[84], C. Austin[55], V. Avendano[85], A. Avila-Alvarez[78], S. Babak[79,86], P. Bacon[79], F. Badaracco[67,68], M. K. M. Bader[87], S. Bae[88], P. T. Baker[89], F. Baldaccini[90,91], G. Ballardin[92], S. W. Ballmer[93], S. Banagiri[94], J. C. Barayoga[54], S. E. Barclay[95], B. C. Barish[54], D. Barker[96], K. Barkett[97], S. Barnum[65], F. Barone[57,58], B. Barr[95], L. Barsotti[65], M. Barsuglia[79], D. Barta[98], J. Bartlett[96], I. Bartos[99], R. Bassiri[100], A. Basti[71,72], M. Bawaj[91,101], J. C. Bayley[95], M. Bazzan[102,103], B. Bécsy[104], M. Bejger[79,105], A. S. Bell[95], D. Beniwal[106], G. Bergmann[61,62], S. Bernuzzi[107,108], J. J. Bero[109], C. P. L. Berry[110], D. Bersanetti[111], A. Bertolini[87], J. Betzwieser[60], R. Bhandare[112], J. Bidler[78], I. A. Bilenko[113], S. A. Bilgili[89], G. Billingsley[54], J. Birch[60], R. Birney[77], O. Birnholtz[109], S. Biscans[54,65], S. Biscoveanu[59], A. Bisht[62], M. Bitossi[72,92], J. K. Blackburn[54], C. D. Blair[60], D. G. Blair[114], R. M. Blair[96], S. Bloemen[115], N. Bode[61,62], M. Boer[116], Y. Boetzel[117], G. Bogaert[116], F. Bondu[118], E. Bonilla[100], R. Bonnand[83], P. Booker[61,62], B. A. Boom[87], C. D. Booth[119], R. Bork[54], V. Boschi[92], S. Bose[56,120], K. Bossie[60], V. Bossilkov[114], J. Bosveld[114], Y. Bouffanais[79], A. Bozzi[92], C. Bradaschia[72], P. R. Brady[76], A. Bramley[60], M. Branchesi[67,68], J. E. Brau[121], T. Briant[122], J. H. Briggs[95], F. Brighenti[123,124], A. Brillet[116], M. Brinkmann[61,62], P. Brockill[76], A. F. Brooks[54], D. D. Brown[106], S. Brunett[54], A. Buikema[65], T. Bulik[125], H. J. Bulten[87,126], A. Buonanno[86,127], D. Buskulic[83], C. Buy[79], R. L. Byer[100], M. Cabero[61,62], L. Cadonati[128], G. Cagnoli[75,129], C. Cahillane[54], J. Calderón Bustillo[59], T. A. Callister[54], E. Calloni[58,130], J. B. Camp[131], W. A. Campbell[59], K. C. Cannon[132], H. Cao[106], J. Cao[133], E. Capocasa[79], F. Carbognani[92], S. Caride[134], M. F. Carney[110], G. Carullo[71], J. Casanueva Diaz[72], C. Casentini[80,81], S. Caudill[87], M. Cavaglià[135], R. Cavalieri[92], G. Cella[72], P. Cerdá-Durán[73], G. Cerretani[71,72], E. Cesarini[81,136], O. Chaibi[116], K. Chakravarti[56], S. J. Chamberlin[137], M. Chan[95], S. Chao[138], P. Charlton[139], E. A. Chase[110], E. Chassande-Mottin[79], D. Chatterjee[76], M. Chaturvedi[112], K. Chatziioannou[140], B. D. Cheeseboro[89], X. Chen[114], Y. Chen[97], H.-P. Cheng[99], C. K. Cheong[141], H. Y. Chia[99], A. Chincarini[111], A. Chiummo[92], G. Cho[142], H. S. Cho[143], M. Cho[127], N. Christensen[116,144], Q. Chu[114], S. Chua[122], K. W. Chung[141], S. Chung[114], G. Ciani[102,103], A. A. Ciobanu[106], R. Ciolfi[145,146], F. Cipriano[116], A. Cirone[111,147], F. Clara[96], J. A. Clark[128], P. Clearwater[148], F. Cleva[116], C. Cocchieri[135], E. Coccia[67,68], P.-F. Cohadon[122], R. Colgan[149], M. Colleoni[150], C. G. Collette[151], C. Collins[64], L. R. Cominsky[152], M. Constancio, Jr.[66], L. Conti[103], S. J. Cooper[64], P. Corban[60], T. R. Corbitt[55], I. Cordero-Carrión[153], K. R. Corley[149], N. Cornish[104], A. Corsi[134], S. Cortese[92], C. A. Costa[66], R. Cotesta[86], M. W. Coughlin[54], S. B. Coughlin[110,119], J.-P. Coulon[116], S. T. Countryman[149], P. Couvares[54], P. B. Covas[150], E. E. Cowan[128], D. M. Coward[114], M. J. Cowart[60], D. C. Coyne[54], R. Coyne[154], J. D. E. Creighton[76], T. D. Creighton[155], J. Cripe[55], M. Croquette[122], S. G. Crowder[156], T. J. Cullen[55], A. Cumming[95], L. Cunningham[95], E. Cuoco[92], T. Dal Canton[131], G. Dálya[157], S. L. Danilishin[61,62], S. D'Antonio[81], K. Danzmann[61,62], A. Dasgupta[158], C. F. Da Silva Costa[99], L. E. H. Datrier[95], V. Dattilo[92], I. Dave[112], D. Davis[93], E. J. Daw[159], D. DeBra[100], M. Deenadayalan[56], J. Degallaix[75], M. De Laurentis[58,130], S. Deléglise[122], W. Del Pozzo[71,72], L. M. DeMarchi[110], N. Demos[65], T. Dent[61,62,160], R. De Pietri[108,161], J. Derby[78], R. De Rosa[58,130], C. De Rossi[75,92], R. DeSalvo[162], O. de Varona[61,62], S. Dhurandhar[56], M. C. Díaz[155], T. Dietrich[87], L. Di Fiore[58], M. Di Giovanni[146,163], T. Di Girolamo[58,130], A. Di Lieto[71,72], B. Ding[151], S. Di Pace[82,164], I. Di Palma[82,164], F. Di Renzo[71,72], A. Dmitriev[64], F. Donovan[65], K. L. Dooley[119,135], S. Doravari[61,62], I. Dorrington[119], T. P. Downes[76], M. Drago[67,68], J. C. Driggers[96], Z. Du[133], P. Dupej[95], S. E. Dwyer[96], P. J. Easter[59], T. B. Edo[159], M. C. Edwards[144], A. Effler[60], P. Ehrens[54],

J. Eichholz[54], S. S. Eikenberry[99], M. Eisenmann[83], R. A. Eisenstein[65], H. Estelles[150], D. Estevez[83], Z. B. Etienne[89], T. Etzel[54], M. Evans[65], T. M. Evans[60], V. Fafone[67,80,81], H. Fair[93], S. Fairhurst[119], X. Fan[133], S. Farinon[111], B. Farr[121], W. M. Farr[64], E. J. Fauchon-Jones[119], M. Favata[85], M. Fays[159], M. Fazio[165], C. Fee[166], J. Feicht[54], M. M. Fejer[100], F. Feng[79], A. Fernandez-Galiana[65], I. Ferrante[71,72], E. C. Ferreira[66], T. A. Ferreira[66], F. Ferrini[92], F. Fidecaro[71,72], I. Fiori[92], D. Fiorucci[79], R. P. Fisher[93,167], J. M. Fishner[65], M. Fitz-Axen[94], R. Flaminio[83,168], M. Fletcher[95], E. Flynn[78], H. Fong[140], J. A. Font[73,169], P. W. F. Forsyth[74], J.-D. Fournier[116], S. Frasca[82,164], F. Frasconi[72], Z. Frei[157], A. Freise[64], R. Frey[121], P. Fritschel[65], V. V. Frolov[60], P. Fulda[99], M. Fyffe[60], H. A. Gabbard[95], B. U. Gadre[56], S. M. Gaebel[64], J. R. Gair[170], L. Gammaitoni[90], M. R. Ganija[106], S. G. Gaonkar[56], A. Garcia[78], C. García-Quirós[150], F. Garufi[58,130], B. Gateley[96], S. Gaudio[84], G. Gaur[171], V. Gayathri[172], G. Gemme[111], E. Genin[92], A. Gennai[72], D. George[70], J. George[112], L. Gergely[173], V. Germain[83], S. Ghonge[128], Abhirup Ghosh[69], Archisman Ghosh[87], S. Ghosh[76], B. Giacomazzo[146,163], J. A. Giaime[55,60], K. D. Giardina[60], A. Giazotto[72,228], K. Gill[84], G. Giordano[57,58], L. Glover[162], P. Godwin[137], E. Goetz[96], R. Goetz[99], B. Goncharov[59], G. González[55], J. M. Gonzalez Castro[71,72], A. Gopakumar[174], M. L. Gorodetsky[113], S. E. Gossan[54], M. Gosselin[92], R. Gouaty[83], A. Grado[58,175], C. Graef[95], M. Granata[75], A. Grant[95], S. Gras[65], P. Grassia[54], C. Gray[96], R. Gray[95], G. Greco[123,124], A. C. Green[64,99], R. Green[119], E. M. Gretarsson[84], P. Groot[115], H. Grote[119], S. Grunewald[86], G. M. Guidi[123,124], H. K. Gulati[158], Y. Guo[87], A. Gupta[137], M. K. Gupta[158], E. K. Gustafson[54], R. Gustafson[176], L. Haegel[150], O. Halim[67,68], B. R. Hall[120], E. D. Hall[65], E. Z. Hamilton[119], G. Hammond[95], M. Haney[117], M. M. Hanke[61,62], J. Hanks[96], C. Hanna[137], O. A. Hannuksela[141], J. Hanson[60], T. Hardwick[55], K. Haris[69], J. Harms[67,68], G. M. Harry[177], I. W. Harry[86], C.-J. Haster[140], K. Haughian[95], F. J. Hayes[95], J. Healy[109], A. Heidmann[122], M. C. Heintze[60], H. Heitmann[116], G. Hemming[92], M. Hendry[95], I. S. Heng[95], J. Hennig[61,62], A. W. Heptonstall[54], Francisco Hernandez Vivanco[59], M. Heurs[61,62], S. Hild[95], T. Hinderer[87,178,179], D. Hoak[92], S. Hochheim[61,62], D. Hofman[75], A. M. Holgado[70], N. A. Holland[74], K. Holt[60], P. Hopkins[119], C. Horst[76], J. Hough[95], E. J. Howell[114], C. G. Hoy[119], A. Hreibi[116], E. A. Huerta[70], B. Hughey[84], M. Hulko[54], S. Husa[150], S. H. Huttner[95], T. Huynh-Dinh[60], B. Idzkowski[125], A. Iess[80,81], C. Ingram[106], R. Inta[134], G. Intini[82,164], B. Irwin[166], H. N. Isa[95], J.-M. Isac[122], M. Isi[54], B. R. Iyer[69], K. Izumi[96], T. Jacqmin[122], S. J. Jadhav[180], K. Jani[128], N. N. Janthalur[180], P. Jaranowski[181], A. C. Jenkins[182], J. Jiang[99], D. S. Johnson[70], A. W. Jones[64], D. I. Jones[183], R. Jones[95], R. J. G. Jonker[87], L. Ju[114], J. Junker[61,62], C. V. Kalaghatgi[119], V. Kalogera[110], B. Kamai[54], S. Kandhasamy[135], G. Kang[88], J. B. Kanner[54], S. J. Kapadia[76], S. Karki[121], K. S. Karvinen[61,62], R. Kashyap[69], M. Kasprzack[54], S. Katsanevas[92], E. Katsavounidis[65], W. Katzman[60], S. Kaufer[62], K. Kawabe[96], N. V. Keerthana[56], F. Kéfélian[116], D. Keitel[95], R. Kennedy[159], J. S. Key[184], F. Y. Khalili[113], H. Khan[78], I. Khan[67,81], S. Khan[61,62], Z. Khan[158], E. A. Khazanov[185], M. Khursheed[112], N. Kijbunchoo[74], Chunglee Kim[186], J. C. Kim[187], K. Kim[141], W. Kim[106], W. S. Kim[188], Y.-M. Kim[189], C. Kimball[110], E. J. King[106], P. J. King[96], M. Kinley-Hanlon[177], R. Kirchhoff[61,62], J. S. Kissel[96], L. Kleybolte[190], J. H. Klika[76], S. Klimenko[99], T. D. Knowles[89], P. Koch[61,62], S. M. Koehlenbeck[61,62], G. Koekoek[87,191], S. Koley[87], V. Kondrashov[54], A. Kontos[65], N. Koper[61,62], M. Korobko[190], W. Z. Korth[54], I. Kowalska[125], D. B. Kozak[54], V. Kringel[61,62], N. Krishnendu[192], A. Królak[193,194], G. Kuehn[61,62], A. Kumar[180], P. Kumar[195], R. Kumar[158], S. Kumar[69], L. Kuo[138], A. Kutynia[193], S. Kwang[76], B. D. Lackey[86], K. H. Lai[141], T. L. Lam[141], M. Landry[96], B. B. Lane[65], R. N. Lang[196], J. Lange[109], B. Lantz[100], R. K. Lanza[65], P. D. Lasky[59], M. Laxen[60], A. Lazzarini[54], C. Lazzaro[103], P. Leaci[82,164], S. Leavey[61,62], Y. K. Lecoeuche[96], C. H. Lee[143], H. K. Lee[197], H. M. Lee[198], H. W. Lee[187], J. Lee[142], K. Lee[95], J. Lehmann[61,62], A. Lenon[89], N. Letendre[83], Y. Levin[59,149], J. Li[133], K. J. L. Li[141], T. G. F. Li[141], X. Li[97], F. Lin[59], F. Linde[87], S. D. Linker[162], T. B. Littenberg[199], J. Liu[114], X. Liu[76], R. K. L. Lo[54,141], N. A. Lockerbie[77], L. T. London[119], A. Longo[200,201], M. Lorenzini[67,68], V. Loriette[202], M. Lormand[60], G. Losurdo[72], J. D. Lough[61,62], C. O. Lousto[109], G. Lovelace[78], M. E. Lower[203], H. Lück[61,62], D. Lumaca[80,81], A. P. Lundgren[204], R. Lynch[65], Y. Ma[97], R. Macas[119], S. Macfoy[77], M. MacInnis[65], D. M. Macleod[119], A. Macquet[116], I. Magaña Hernandez[76], F. Magaña-Sandoval[93], L. Magaña Zertuche[135], R. M. Magee[137], E. Majorana[82], I. Maksimovic[202], A. Malik[112], N. Man[116], V. Mandic[94], V. Mangano[95], G. L. Mansell[65,96], M. Manske[74,76], M. Mantovani[92], F. Marchesoni[91,101], F. Marion[83], S. Márka[149], Z. Márka[149], C. Markakis[63,70], A. S. Markosyan[100], A. Markowitz[54], E. Maros[54], A. Marquina[153], S. Marsat[86], F. Martelli[123,124], I. W. Martin[95], R. M. Martin[85], D. V. Martynov[64], K. Mason[65], E. Massera[159], A. Masserot[83], T. J. Massinger[54], M. Masso-Reid[95], S. Mastrogiovanni[82,164], A. Matas[86,94], F. Matichard[54,65], L. Matone[149], N. Mavalvala[65], N. Mazumder[120], J. J. McCann[114], R. McCarthy[96], D. E. McClelland[74], S. McCormick[60], L. McCuller[65], S. C. McGuire[205], J. McIver[54], D. J. McManus[74], T. McRae[74], S. T. McWilliams[89], D. Meacher[137], G. D. Meadors[59], M. Mehmet[61,62], A. K. Mehta[69], J. Meidam[87], A. Melatos[148], G. Mendell[96], R. A. Mercer[76], L. Mereni[75], E. L. Merilh[96], M. Merzougui[116], S. Meshkov[54], C. Messenger[95], C. Messick[137], R. Metzdorff[122], P. M. Meyers[148], H. Miao[64], C. Michel[75], H. Middleton[148], E. E. Mikhailov[206], L. Milano[58,130], A. L. Miller[99], A. Miller[82,164], M. Millhouse[104], J. C. Mills[119], M. C. Milovich-Goff[162], O. Minazzoli[116,207], Y. Minenkov[81], A. Mishkin[99], C. Mishra[208], T. Mistry[159], S. Mitra[56], V. P. Mitrofanov[113], G. Mitselmakher[99], R. Mittleman[65], G. Mo[144], D. Moffa[166], K. Mogushi[135], S. R. P. Mohapatra[65], M. Montani[123,124], C. J. Moore[63], D. Moraru[96], G. Moreno[96], S. Morisaki[132], B. Mours[83], C. M. Mow-Lowry[64], Arunava Mukherjee[61,62], D. Mukherjee[76], S. Mukherjee[155], N. Mukund[56], A. Mullavey[60], J. Munch[106], E. A. Muñiz[93], M. Muratore[84], P. G. Murray[95], I. Nardecchia[80,81], L. Naticchioni[82,164], R. K. Nayak[209], J. Neilson[162], G. Nelemans[87,115], T. J. N. Nelson[60], M. Nery[61,62], A. Neunzert[176], K. Y. Ng[65], S. Ng[106], P. Nguyen[121], D. Nichols[87,178], S. Nissanke[87,178], F. Nocera[92], C. North[119], L. K. Nuttall[204], M. Obergaulinger[73], J. Oberling[96], B. D. O'Brien[99], G. D. O'Dea[162], G. H. Ogin[210], J. J. Oh[188], S. H. Oh[188], F. Ohme[61,62], H. Ohta[132], M. A. Okada[66], M. Oliver[150], P. Oppermann[61,62], Richard J. Oram[60], B. O'Reilly[60], R. G. Ormiston[94], L. F. Ortega[99], R. O'Shaughnessy[109], S. Ossokine[86], D. J. Ottaway[106],

H. Overmier[60], B. J. Owen[134], A. E. Pace[137], G. Pagano[71,72], M. A. Page[114], A. Pai[172], S. A. Pai[112], J. R. Palamos[121], O. Palashov[185], C. Palomba[82], A. Pal-Singh[190], Huang-Wei Pan[138], B. Pang[97], P. T. H. Pang[141], C. Pankow[110], F. Pannarale[82,164], B. C. Pant[112], F. Paoletti[72], A. Paoli[92], A. Parida[56], W. Parker[60,205], D. Pascucci[95], A. Pasqualetti[92], R. Passaquieti[71,72], D. Passuello[72], M. Patil[194], B. Patricelli[71,72], B. L. Pearlstone[95], C. Pedersen[119], M. Pedraza[54], R. Pedurand[75,211], A. Pele[60], S. Penn[212], C. J. Perez[96], A. Perreca[146,163], H. P. Pfeiffer[86,140], M. Phelps[61,62], K. S. Phukon[56], O. J. Piccinni[82,164], M. Pichot[116], F. Piergiovanni[123,124], G. Pillant[92], L. Pinard[75], M. Pirello[96], M. Pitkin[95], R. Poggiani[71,72], D. Y. T. Pong[141], S. Ponrathnam[56], P. Popolizio[92], E. K. Porter[79], J. Powell[203], A. K. Prajapati[158], J. Prasad[56], K. Prasai[100], R. Prasanna[180], G. Pratten[150], T. Prestegard[76], S. Privitera[86], G. A. Prodi[146,163], L. G. Prokhorov[113], O. Puncken[61,62], M. Punturo[91], P. Puppo[82], M. Pürrer[86], H. Qi[76], V. Quetschke[155], P. J. Quinonez[84], E. A. Quintero[54], R. Quitzow-James[121], H. Radkins[96], N. Radulescu[116], P. Raffai[157], S. Raja[112], C. Rajan[112], B. Rajbhandari[134], M. Rakhmanov[155], K. E. Ramirez[155], A. Ramos-Buades[150], Javed Rana[56], K. Rao[110], P. Rapagnani[82,164], V. Raymond[119], M. Razzano[71,72], J. Read[78], T. Regimbau[83], L. Rei[111], S. Reid[77], D. H. Reitze[54,99], W. Ren[70], F. Ricci[82,164], C. J. Richardson[84], J. W. Richardson[54], P. M. Ricker[70], K. Riles[176], M. Rizzo[110], N. A. Robertson[54,95], R. Robie[95], A. Rocchi[81], L. Rolland[83], J. G. Rollins[54], V. J. Roma[121], M. Romanelli[118], R. Romano[57,58], C. L. Romel[96], J. H. Romie[60], K. Rose[166], D. Rosińska[105,213], S. G. Rosofsky[70], M. P. Ross[214], S. Rowan[95], A. Rüdiger[61,62,229], P. Ruggi[92], G. Rutins[215], K. Ryan[96], S. Sachdev[54], T. Sadecki[96], M. Sakellariadou[182], L. Salconi[92], M. Saleem[192], A. Samajdar[87], L. Sammut[59], E. J. Sanchez[54], L. E. Sanchez[54], N. Sanchis-Gual[73], V. Sandberg[96], J. R. Sanders[93], K. A. Santiago[85], N. Sarin[59], B. Sassolas[75,119], P. R. Saulson[93], O. Sauter[176], R. L. Savage[96], P. Schale[121], M. Scheel[97], J. Scheuer[110], P. Schmidt[115], R. Schnabel[190], R. M. S. Schofield[121], A. Schönbeck[190], E. Schreiber[61,62], B. W. Schulte[61,62], B. F. Schutz[119], S. G. Schwalbe[84], J. Scott[95], S. M. Scott[74], E. Seidel[70], D. Sellers[60], A. S. Sengupta[216], N. Sennett[86], D. Sentenac[92], V. Sequino[67,80,81], A. Sergeev[185], D. A. Shaddock[74], T. Shaffer[96], M. S. Shahriar[110], M. B. Shaner[162], L. Shao[86], P. Sharma[112], P. Shawhan[127], H. Shen[70], R. Shink[217], D. H. Shoemaker[65], D. M. Shoemaker[128], S. ShyamSundar[112], K. Siellez[128], M. Sieniawska[105], D. Sigg[96], A. D. Silva[66], L. P. Singer[131], N. Singh[125], A. Singhal[67,82], A. M. Sintes[150], S. Sitmukhambetov[155], V. Skliris[119], B. J. J. Slagmolen[74], T. J. Slaven-Blair[114], J. R. Smith[78], R. J. E. Smith[59], S. Somala[218], E. J. Son[188], B. Sorazu[95], F. Sorrentino[111], T. Souradeep[56], E. Sowell[134], A. P. Spencer[95], A. K. Srivastava[158], V. Srivastava[93], K. Staats[110], C. Stachie[116], M. Standke[61,62], D. A. Steer[79], M. Steinke[61,62], J. Steinlechner[95,190], S. Steinlechner[190], D. Steinmeyer[61,62], S. P. Stevenson[203], D. Stocks[100], R. Stone[155], D. J. Stops[64], K. A. Strain[95], G. Stratta[123,124], S. E. Strigin[113], A. Strunk[96], R. Sturani[219], A. L. Stuver[220], V. Sudhir[65], T. Z. Summerscales[221], L. Sun[54], S. Sunil[158], A. Sur[87,105], J. Suresh[56], P. J. Sutton[119], B. L. Swinkels[87], M. J. Szczepańczyk[84], M. Tacca[87], S. C. Tait[95], C. Talbot[59], D. Talukder[121], D. B. Tanner[99], M. Tápai[173], A. Taracchini[86], J. D. Tasson[144], R. Taylor[54], F. Thies[61,62], M. Thomas[60], P. Thomas[96], S. R. Thondapu[112], K. A. Thorne[60], E. Thrane[59], Shubhanshu Tiwari[146,163], Srishti Tiwari[174], V. Tiwari[119], K. Toland[95], M. Tonelli[71,72], Z. Tornasi[95], A. Torres-Forné[222], C. I. Torrie[54], D. Töyrä[64], F. Travasso[91,92], G. Traylor[60], M. C. Tringali[125], A. Trovato[79], L. Trozzo[72,223], R. Trudeau[54], K. W. Tsang[87], M. Tse[65], R. Tso[97], L. Tsukada[132], D. Tsuna[132], D. Tuyenbayev[155], K. Ueno[132], D. Ugolini[224], C. S. Unnikrishnan[174], A. L. Urban[55], S. A. Usman[119], H. Vahlbruch[62], G. Vajente[54], G. Valdes[55], N. van Bakel[87], M. van Beuzekom[87], J. F. J. van den Brand[87,126], C. Van Den Broeck[87,225], D. C. Vander-Hyde[93], J. V. van Heijningen[114], L. van der Schaaf[87], A. A. van Veggel[95], M. Vardaro[102,103], V. Varma[97], S. Vass[54], M. Vasúth[98], A. Vecchio[64], G. Vedovato[103], J. Veitch[95], P. J. Veitch[106], K. Venkateswara[214], G. Venugopalan[54], D. Verkindt[83], F. Vetrano[123,124], A. Viceré[123,124], A. D. Viets[76], D. J. Vine[215], J.-Y. Vinet[116], S. Vitale[65], T. Vo[93], H. Vocca[90,91], C. Vorvick[96], S. P. Vyatchanin[113], A. R. Wade[54], L. E. Wade[166], M. Wade[166], R. Walet[87], M. Walker[78], L. Wallace[54], S. Walsh[76], G. Wang[67,72], H. Wang[64], J. Z. Wang[176], W. H. Wang[155], Y. F. Wang[141], R. L. Ward[74], Z. A. Warden[84], J. Warner[96], M. Was[83], J. Watchi[151], B. Weaver[96], L.-W. Wei[61,62], M. Weinert[61,62], A. J. Weinstein[54], R. Weiss[65], F. Wellmann[61,62], L. Wen[114], E. K. Wessel[70], P. Weßels[61,62], J. W. Westhouse[84], K. Wette[74], J. T. Whelan[109], B. F. Whiting[99], C. Whittle[65], D. M. Wilken[61,62], D. Williams[95], A. R. Williamson[87,178], J. L. Willis[54], B. Willke[61,62], M. H. Wimmer[61,62], W. Winkler[61,62], C. C. Wipf[54], H. Wittel[61,62], G. Woan[95], J. Woehler[61,62], J. K. Wofford[109], J. Worden[96], J. L. Wright[95], D. S. Wu[61,62], D. M. Wysocki[109], L. Xiao[54], H. Yamamoto[54], C. C. Yancey[127], L. Yang[165], M. J. Yap[74], M. Yazback[99], D. W. Yeeles[119], Hang Yu[65], Haocun Yu[65], S. H. R. Yuen[141], M. Yvert[83], A. K. Zadrożny[155,193], M. Zanolin[84], T. Zelenova[92], J.-P. Zendri[103], M. Zevin[110], J. Zhang[114], L. Zhang[54], T. Zhang[95], C. Zhao[114], M. Zhou[110], Z. Zhou[110], X. J. Zhu[59], A. Zimmerman[226], M. E. Zucker[54,65], and J. Zweizig[54]

(The LIGO Scientific Collaboration and the Virgo Collaboration)

[1] Department of Physics, Brandeis University, Waltham, MA 02453, USA
[2] Fermi National Accelerator Laboratory, P.O. Box 500, Batavia, IL 60510, USA; palmese@fnal.gov
[3] Department of Physics & Astronomy, University College London, Gower Street, London WC1E 6BT, UK
[4] Instituto de Fisica Teorica UAM/CSIC, Universidad Autonoma de Madrid, E-28049 Madrid, Spain
[5] Department of Physics, University of Chicago, Chicago, IL 60637, USA
[6] Kavli Institute for Cosmological Physics, University of Chicago, Chicago, IL 60637, USA
[7] University of Chicago, Chicago, IL 60637, USA
[8] Department of Astronomy and Astrophysics, University of Chicago, Chicago, IL 60637, USA
[9] Department of Physics and Astronomy, University of Pennsylvania, Philadelphia, PA 19104, USA
[10] Centro de Investigaciones Energéticas, Medioambientales y Tecnológicas (CIEMAT), Madrid, Spain
[11] Laboratório Interinstitucional de e-Astronomia—LIneA, Rua Gal. José Cristino 77, Rio de Janeiro, RJ—20921-400, Brazil
[12] University of Nottingham, School of Physics and Astronomy, Nottingham NG7 2RD, UK
[13] Kavli Institute for Particle Astrophysics and Cosmology and Department of Physics, Stanford University, Stanford, CA 94305, USA

[14] Department of Particle Physics & Astrophysics, SLAC National Accelerator Laboratory, Menlo Park, CA 94025, USA
[15] SLAC National Accelerator Laboratory, Menlo Park, CA 94025, USA
[16] Observatório Nacional, Rua Gal. José Cristino 77, Rio de Janeiro, RJ—20921-400, Brazil
[17] Department of Physics, Stanford University, 382 Via Pueblo Mall, Stanford, CA 94305, USA
[18] Kavli Institute for Particle Astrophysics & Cosmology, P.O. Box 2450, Stanford University, Stanford, CA 94305, USA
[19] Harvard-Smithsonian Center for Astrophysics, 60 Garden Street, Cambridge MA 02138, USA
[20] The Observatories of the Carnegie Institution for Science, 813 Santa Barbara Street, Pasadena, CA 91101, USA
[21] Department of Physics, Columbia University, New York, NY 10025, USA
[22] American Astronomical Society, 1667 K Street NW, Suite 800, Washington, DC 20006, USA
[23] Cerro Tololo Inter-American Observatory, National Optical Astronomy Observatory, Casilla 603, La Serena, Chile
[24] Institute of Cosmology and Gravitation, University Of Portsmouth, Portsmouth PO1 3FX, UK
[25] LSST, 933 North Cherry Avenue, Tucson, AZ 85721, USA
[26] Physics Department, 2320 Chamberlin Hall, University of Wisconsin-Madison, 1150 University Avenue Madison, WI 53706-1390, USA
[27] CNRS, UMR 7095, Institut d'Astrophysique de Paris, F-75014, Paris, France
[28] Sorbonne Universités, UPMC Univ Paris 06, UMR 7095, Institut d'Astrophysique de Paris, F-75014, Paris, France
[29] Department of Astronomy, University of Illinois at Urbana-Champaign, 1002 West Green Street, Urbana, IL 61801, USA
[30] National Center for Supercomputing Applications, 1205 West Clark Street, Urbana, IL 61801, USA
[31] Institut de Física d'Altes Energies (IFAE), The Barcelona Institute of Science and Technology, Campus UAB, E-08193 Bellaterra (Barcelona), Spain
[32] Institut d'Estudis Espacials de Catalunya (IEEC), E-08034 Barcelona, Spain
[33] Institute of Space Sciences (*ICE*, CSIC), Campus UAB, Carrer de Can Magrans, s/n, E-08193 Barcelona, Spain
[34] Department of Physics, IIT Hyderabad, Kandi, Telangana 502285, India
[35] Department of Astronomy/Steward Observatory, 933 North Cherry Avenue, Tucson, AZ 85721-0065, USA
[36] Jet Propulsion Laboratory, California Institute of Technology, 4800 Oak Grove Dr., Pasadena, CA 91109, USA
[37] Department of Astronomy, University of Michigan, Ann Arbor, MI 48109, USA
[38] Department of Physics, University of Michigan, Ann Arbor, MI 48109, USA
[39] Santa Cruz Institute for Particle Physics, Santa Cruz, CA 95064, USA
[40] Max Planck Institute for Extraterrestrial Physics, Giessenbachstrasse, D-85748 Garching, Germany
[41] Universitäts-Sternwarte, Fakultät für Physik, Ludwig-Maximilians Universität München, Scheinerstr. 1, D-81679 München, Germany
[42] Harvard-Smithsonian Center for Astrophysics, Cambridge, MA 02138, USA
[43] Australian Astronomical Optics, Macquarie University, North Ryde, NSW 2113, Australia
[44] Departamento de Física Matemática, Instituto de Física, Universidade de São Paulo, CP 66318, São Paulo, SP, 05314-970, Brazil
[45] George P. and Cynthia Woods Mitchell Institute for Fundamental Physics and Astronomy, and Department of Physics and Astronomy, Texas A&M University, College Station, TX 77843, USA
[46] Institució Catalana de Recerca i Estudis Avançats, E-08010 Barcelona, Spain
[47] Department of Astrophysical Sciences, Princeton University, 4 Ivy Lane, Princeton, NJ 08544, USA
[48] Department of Physics and Astronomy, Pevensey Building, University of Sussex, Brighton BN1 9QH, UK
[49] School of Physics and Astronomy, University of Southampton, Southampton, SO17 1BJ, UK
[50] Instituto de Física Gleb Wataghin, Universidade Estadual de Campinas, 13083-859, Campinas, SP, Brazil
[51] Computer Science and Mathematics Division, Oak Ridge National Laboratory, Oak Ridge, TN 37831, USA
[52] Lawrence Berkeley National Laboratory, 1 Cyclotron Road, Berkeley, CA 94720, USA
[53] Institute for Astronomy, University of Edinburgh, Edinburgh EH9 3HJ, UK
[54] LIGO, California Institute of Technology, Pasadena, CA 91125, USA
[55] Louisiana State University, Baton Rouge, LA 70803, USA
[56] Inter-University Centre for Astronomy and Astrophysics, Pune 411007, India
[57] Università di Salerno, Fisciano, I-84084 Salerno, Italy
[58] INFN, Sezione di Napoli, Complesso Universitario di Monte S. Angelo, I-80126 Napoli, Italy
[59] OzGrav, School of Physics & Astronomy, Monash University, Clayton 3800, Victoria, Australia
[60] LIGO Livingston Observatory, Livingston, LA 70754, USA
[61] Max Planck Institute for Gravitational Physics (Albert Einstein Institute), D-30167 Hannover, Germany
[62] Leibniz Universität Hannover, D-30167 Hannover, Germany
[63] University of Cambridge, Cambridge CB2 1TN, UK
[64] University of Birmingham, Birmingham B15 2TT, UK
[65] LIGO, Massachusetts Institute of Technology, Cambridge, MA 02139, USA
[66] Instituto Nacional de Pesquisas Espaciais, 12227-010 São José dos Campos, São Paulo, Brazil
[67] Gran Sasso Science Institute (GSSI), I-67100 L'Aquila, Italy
[68] INFN, Laboratori Nazionali del Gran Sasso, I-67100 Assergi, Italy
[69] International Centre for Theoretical Sciences, Tata Institute of Fundamental Research, Bengaluru 560089, India
[70] NCSA, University of Illinois at Urbana-Champaign, Urbana, IL 61801, USA
[71] Università di Pisa, I-56127 Pisa, Italy
[72] INFN, Sezione di Pisa, I-56127 Pisa, Italy
[73] Departamento de Astronomía y Astrofísica, Universitat de València, E-46100 Burjassot, València, Spain
[74] OzGrav, Australian National University, Canberra, Australian Capital Territory 0200, Australia
[75] Laboratoire des Matériaux Avancés (LMA), CNRS/IN2P3, F-69622 Villeurbanne, France
[76] University of Wisconsin-Milwaukee, Milwaukee, WI 53201, USA
[77] SUPA, University of Strathclyde, Glasgow G1 1XQ, UK
[78] California State University Fullerton, Fullerton, CA 92831, USA
[79] APC, AstroParticule et Cosmologie, Université Paris Diderot, CNRS/IN2P3, CEA/Irfu, Observatoire de Paris, Sorbonne Paris Cité, F-75205 Paris Cedex 13, France
[80] Università di Roma Tor Vergata, I-00133 Roma, Italy
[81] INFN, Sezione di Roma Tor Vergata, I-00133 Roma, Italy
[82] INFN, Sezione di Roma, I-00185 Roma, Italy
[83] Laboratoire d'Annecy de Physique des Particules (LAPP), Univ. Grenoble Alpes, Université Savoie Mont Blanc, CNRS/IN2P3, F-74941 Annecy, France
[84] Embry-Riddle Aeronautical University, Prescott, AZ 86301, USA
[85] Montclair State University, Montclair, NJ 07043, USA
[86] Max Planck Institute for Gravitational Physics (Albert Einstein Institute), D-14476 Potsdam-Golm, Germany
[87] Nikhef, Science Park 105, 1098 XG Amsterdam, The Netherlands

[88] Korea Institute of Science and Technology Information, Daejeon 34141, Republic of Korea
[89] West Virginia University, Morgantown, WV 26506, USA
[90] Università di Perugia, I-06123 Perugia, Italy
[91] INFN, Sezione di Perugia, I-06123 Perugia, Italy
[92] European Gravitational Observatory (EGO), I-56021 Cascina, Pisa, Italy
[93] Syracuse University, Syracuse, NY 13244, USA
[94] University of Minnesota, Minneapolis, MN 55455, USA
[95] SUPA, University of Glasgow, Glasgow G12 8QQ, UK
[96] LIGO Hanford Observatory, Richland, WA 99352, USA
[97] Caltech CaRT, Pasadena, CA 91125, USA
[98] Wigner RCP, RMKI, H-1121 Budapest, Konkoly Thege Miklós út 29-33, Hungary
[99] University of Florida, Gainesville, FL 32611, USA
[100] Stanford University, Stanford, CA 94305, USA
[101] Università di Camerino, Dipartimento di Fisica, I-62032 Camerino, Italy
[102] Università di Padova, Dipartimento di Fisica e Astronomia, I-35131 Padova, Italy
[103] INFN, Sezione di Padova, I-35131 Padova, Italy
[104] Montana State University, Bozeman, MT 59717, USA
[105] Nicolaus Copernicus Astronomical Center, Polish Academy of Sciences, 00-716, Warsaw, Poland
[106] OzGrav, University of Adelaide, Adelaide, South Australia 5005, Australia
[107] Theoretisch-Physikalisches Institut, Friedrich-Schiller-Universität Jena, D-07743 Jena, Germany
[108] INFN, Sezione di Milano Bicocca, Gruppo Collegato di Parma, I-43124 Parma, Italy
[109] Rochester Institute of Technology, Rochester, NY 14623, USA
[110] Center for Interdisciplinary Exploration & Research in Astrophysics (CIERA), Northwestern University, Evanston, IL 60208, USA
[111] INFN, Sezione di Genova, I-16146 Genova, Italy
[112] RRCAT, Indore, Madhya Pradesh 452013, India
[113] Faculty of Physics, Lomonosov Moscow State University, Moscow 119991, Russia
[114] OzGrav, University of Western Australia, Crawley, Western Australia 6009, Australia
[115] Department of Astrophysics/IMAPP, Radboud University Nijmegen, P.O. Box 9010, 6500 GL Nijmegen, The Netherlands
[116] Artemis, Université Côte d'Azur, Observatoire Côte d'Azur, CNRS, CS 34229, F-06304 Nice Cedex 4, France
[117] Physik-Institut, University of Zurich, Winterthurerstrasse 190, 8057 Zurich, Switzerland
[118] Univ Rennes, CNRS, Institut FOTON—UMR6082, F-3500 Rennes, France
[119] Cardiff University, Cardiff CF24 3AA, UK
[120] Washington State University, Pullman, WA 99164, USA
[121] University of Oregon, Eugene, OR 97403, USA
[122] Laboratoire Kastler Brossel, Sorbonne Université, CNRS, ENS-Université PSL, Collège de France, F-75005 Paris, France
[123] Università degli Studi di Urbino "Carlo Bo," I-61029 Urbino, Italy
[124] INFN, Sezione di Firenze, I-50019 Sesto Fiorentino, Firenze, Italy
[125] Astronomical Observatory Warsaw University, 00-478 Warsaw, Poland
[126] VU University Amsterdam, 1081 HV Amsterdam, The Netherlands
[127] University of Maryland, College Park, MD 20742, USA
[128] School of Physics, Georgia Institute of Technology, Atlanta, GA 30332, USA
[129] Université Claude Bernard Lyon 1, F-69622 Villeurbanne, France
[130] Università di Napoli "Federico II," Complesso Universitario di Monte S.Angelo, I-80126 Napoli, Italy
[131] NASA Goddard Space Flight Center, Greenbelt, MD 20771, USA
[132] RESCEU, University of Tokyo, Tokyo, 113-0033, Japan
[133] Tsinghua University, Beijing 100084, People's Republic of China
[134] Texas Tech University, Lubbock, TX 79409, USA
[135] The University of Mississippi, University, MS 38677, USA
[136] Museo Storico della Fisica e Centro Studi e Ricerche "Enrico Fermi," I-00184 Roma, Italy
[137] The Pennsylvania State University, University Park, PA 16802, USA
[138] National Tsing Hua University, Hsinchu City, 30013 Taiwan, Republic of People's Republic of China
[139] Charles Sturt University, Wagga Wagga, New South Wales 2678, Australia
[140] Canadian Institute for Theoretical Astrophysics, University of Toronto, Toronto, ON M5S 3H8, Canada
[141] The Chinese University of Hong Kong, Shatin, NT, Hong Kong
[142] Seoul National University, Seoul 08826, Republic of Korea
[143] Pusan National University, Busan 46241, Republic of Korea
[144] Carleton College, Northfield, MN 55057, USA
[145] INAF, Osservatorio Astronomico di Padova, I-35122 Padova, Italy
[146] INFN, Trento Institute for Fundamental Physics and Applications, I-38123 Povo, Trento, Italy
[147] Dipartimento di Fisica, Università degli Studi di Genova, I-16146 Genova, Italy
[148] OzGrav, University of Melbourne, Parkville, Victoria 3010, Australia
[149] Columbia University, New York, NY 10027, USA
[150] Universitat de les Illes Balears, IAC3—IEEC, E-07122 Palma de Mallorca, Spain
[151] Université Libre de Bruxelles, Brussels B-1050, Belgium
[152] Sonoma State University, Rohnert Park, CA 94928, USA
[153] Departamento de Matemáticas, Universitat de València, E-46100 Burjassot, València, Spain
[154] University of Rhode Island, Kingston, RI 02881, USA
[155] The University of Texas Rio Grande Valley, Brownsville, TX 78520, USA
[156] Bellevue College, Bellevue, WA 98007, USA
[157] MTA-ELTE Astrophysics Research Group, Institute of Physics, Eötvös University, Budapest 1117, Hungary
[158] Institute for Plasma Research, Bhat, Gandhinagar 382428, India
[159] The University of Sheffield, Sheffield S10 2TN, UK
[160] IGFAE, Campus Sur, Universidade de Santiago de Compostela, E-15782, Spain
[161] Dipartimento di Scienze Matematiche, Fisiche e Informatiche, Università di Parma, I-43124 Parma, Italy
[162] California State University, Los Angeles, 5151 State University Drive, Los Angeles, CA 90032, USA
[163] Università di Trento, Dipartimento di Fisica, I-38123 Povo, Trento, Italy

[164] Università di Roma "La Sapienza," I-00185 Roma, Italy
[165] Colorado State University, Fort Collins, CO 80523, USA
[166] Kenyon College, Gambier, OH 43022, USA
[167] Christopher Newport University, Newport News, VA 23606, USA
[168] National Astronomical Observatory of Japan, 2-21-1 Osawa, Mitaka, Tokyo 181-8588, Japan
[169] Observatori Astronòmic, Universitat de València, E-46980 Paterna, València, Spain
[170] School of Mathematics, University of Edinburgh, Edinburgh EH9 3FD, UK
[171] Institute Of Advanced Research, Gandhinagar 382426, India
[172] Indian Institute of Technology Bombay, Powai, Mumbai 400 076, India
[173] University of Szeged, Dóm tér 9, Szeged 6720, Hungary
[174] Tata Institute of Fundamental Research, Mumbai 400005, India
[175] INAF, Osservatorio Astronomico di Capodimonte, I-80131, Napoli, Italy
[176] University of Michigan, Ann Arbor, MI 48109, USA
[177] American University, Washington, D.C. 20016, USA
[178] GRAPPA, Anton Pannekoek Institute for Astronomy and Institute of High-Energy Physics, University of Amsterdam, Science Park 904, 1098 XH Amsterdam, The Netherlands
[179] Delta Institute for Theoretical Physics, Science Park 904, 1090 GL Amsterdam, The Netherlands
[180] Directorate of Construction, Services & Estate Management, Mumbai 400094, India
[181] University of Białystok, 15-424 Białystok, Poland
[182] King's College London, University of London, London WC2R 2LS, UK
[183] University of Southampton, Southampton SO17 1BJ, UK
[184] University of Washington Bothell, Bothell, WA 98011, USA
[185] Institute of Applied Physics, Nizhny Novgorod, 603950, Russia
[186] Ewha Womans University, Seoul 03760, Republic of Korea
[187] Inje University Gimhae, South Gyeongsang 50834, Republic of Korea
[188] National Institute for Mathematical Sciences, Daejeon 34047, Republic of Korea
[189] Ulsan National Institute of Science and Technology, Ulsan 44919, Republic of Korea
[190] Universität Hamburg, D-22761 Hamburg, Germany
[191] Maastricht University, P.O. Box 616, 6200 MD Maastricht, The Netherlands
[192] Chennai Mathematical Institute, Chennai 603103, India
[193] NCBJ, 05-400 Świerk-Otwock, Poland
[194] Institute of Mathematics, Polish Academy of Sciences, 00656 Warsaw, Poland
[195] Cornell University, Ithaca, NY 14850, USA
[196] Hillsdale College, Hillsdale, MI 49242, USA
[197] Hanyang University, Seoul 04763, Republic of Korea
[198] Korea Astronomy and Space Science Institute, Daejeon 34055, Republic of Korea
[199] NASA Marshall Space Flight Center, Huntsville, AL 35811, USA
[200] Dipartimento di Matematica e Fisica, Università degli Studi Roma Tre, I-00146 Roma, Italy
[201] INFN, Sezione di Roma Tre, I-00146 Roma, Italy
[202] ESPCI, CNRS, F-75005 Paris, France
[203] OzGrav, Swinburne University of Technology, Hawthorn VIC 3122, Australia
[204] University of Portsmouth, Portsmouth PO1 3FX, UK
[205] Southern University and A&M College, Baton Rouge, LA 70813, USA
[206] College of William and Mary, Williamsburg, VA 23187, USA
[207] Centre Scientifique de Monaco, 8 quai Antoine Ier, MC-98000, Monaco
[208] Indian Institute of Technology Madras, Chennai 600036, India
[209] IISER-Kolkata, Mohanpur, West Bengal 741252, India
[210] Whitman College, 345 Boyer Avenue, Walla Walla, WA 99362, USA
[211] Université de Lyon, F-69361 Lyon, France
[212] Hobart and William Smith Colleges, Geneva, NY 14456, USA
[213] Janusz Gil Institute of Astronomy, University of Zielona Góra, 65-265 Zielona Góra, Poland
[214] University of Washington, Seattle, WA 98195, USA
[215] SUPA, University of the West of Scotland, Paisley PA1 2BE, UK
[216] Indian Institute of Technology, Gandhinagar Ahmedabad Gujarat 382424, India
[217] Université de Montréal/Polytechnique, Montreal, QC H3T 1J4, Canada
[218] Indian Institute of Technology Hyderabad, Sangareddy, Khandi, Telangana 502285, India
[219] International Institute of Physics, Universidade Federal do Rio Grande do Norte, Natal RN 59078-970, Brazil
[220] Villanova University, 800 Lancaster Avenue, Villanova, PA 19085, USA
[221] Andrews University, Berrien Springs, MI 49104, USA
[222] Max Planck Institute for Gravitationalphysik (Albert Einstein Institute), D-14476 Potsdam-Golm, Germany
[223] Università di Siena, I-53100 Siena, Italy
[224] Trinity University, San Antonio, TX 78212, USA
[225] Van Swinderen Institute for Particle Physics and Gravity, University of Groningen, Nijenborgh 4, 9747 AG Groningen, The Netherlands
[226] The University of Texas at Austin, Austin, TX 78712, USA
Received 2018 December 21; revised 2019 March 22; accepted 2019 March 31; published 2019 April 26

[227] Hubble Fellow.
[228] Deceased, 2017 November.
[229] Deceased, 2018 July.

Abstract

We present a multi-messenger measurement of the Hubble constant H_0 using the binary–black-hole merger GW170814 as a standard siren, combined with a photometric redshift catalog from the Dark Energy Survey (DES). The luminosity distance is obtained from the gravitational wave signal detected by the Laser Interferometer Gravitational-Wave Observatory (LIGO)/Virgo Collaboration (LVC) on 2017 August 14, and the redshift information is provided by the DES Year 3 data. Black hole mergers such as GW170814 are expected to lack bright electromagnetic emission to uniquely identify their host galaxies and build an object-by-object Hubble diagram. However, they are suitable for a statistical measurement, provided that a galaxy catalog of adequate depth and redshift completion is available. Here we present the first Hubble parameter measurement using a black hole merger. Our analysis results in $H_0 = 75^{+40}_{-32}$ km s^{-1} Mpc^{-1}, which is consistent with both SN Ia and cosmic microwave background measurements of the Hubble constant. The quoted 68% credible region comprises 60% of the uniform prior range [20, 140] km s^{-1} Mpc^{-1}, and it depends on the assumed prior range. If we take a broader prior of [10, 220] km s^{-1} Mpc^{-1}, we find $H_0 = 78^{+96}_{-24}$ km s^{-1} Mpc^{-1} (57% of the prior range). Although a weak constraint on the Hubble constant from a single event is expected using the dark siren method, a multifold increase in the LVC event rate is anticipated in the coming years and combinations of many sirens will lead to improved constraints on H_0.

Key words: catalogs – cosmology: observations – gravitational waves – surveys

1. Introduction

Unlike most extragalactic distance observables, mergers of neutron star and black hole binary systems are absolute distance indicators. Often referred to as "standard sirens," they emit gravitational waves (GWs) from which the luminosity distance can be inferred without relying on any calibration with respect to another source: the rate of change in frequency gives the system's size and thus the intrinsic amplitude, which is compared against the observed signal amplitude to obtain the distance to the source. If redshifts are associated with those sirens (in the simplest case, the host galaxy is identified and its redshift is obtained via spectroscopic follow up), a measurement of the present rate of expansion of the universe H_0 can be achieved via the distance–redshift relation. The use of GW sources as cosmological probes was first proposed by Schutz (1986), and recently revisited in several works (e.g., Holz & Hughes 2005).

For dark energy research, the possibility of measuring H_0 directly and independently from other methods is of great interest. Local measurements obtained from SN Ia and other distance indicators, as well as the predicted value inferred from the cosmic microwave background (CMB) at $z \sim 1100$, have achieved remarkable precision of 1%–2.5% (e.g., Planck Collaboration et al. 2018; Riess et al. 2018). They disagree, however, by more than 3σ and interpreting this tension as evidence for beyond-ΛCDM dark energy or new physics at the early universe requires new measurements of great precision and accuracy (Freedman 2017; Mörtsell & Dhawan 2018). Those measurements are one of the greatest challenges faced by current experiments in cosmology because the observables are subject to correlated systematic effects arising from their complex astrophysics. As estimates become more precise, this challenge becomes more severe and the need for novel independent methods becomes more pressing. Those methods, however, are few and hard to come by. One possibility is standard sirens, which remained elusive for almost 30 yr, until the detection of the first GW event (GW150914; Abbott et al. 2016). The first standard siren-based H_0 measurement (Abbott et al. 2017a) came with the discovery of the binary–neutron-star (BNS) merger GW170817 (Abbott et al. 2017) and its associated electromagnetic counterpart (Arcavi et al. 2017; Coulter et al. 2017; LIGO Scientific Collaboration et al. 2017; Lipunov et al. 2017; Soares-Santos et al. 2017; Tanvir et al. 2017; Valenti et al. 2017). Several studies have developed methodologies to infer cosmological parameters from standard sirens and establish their constraining power (Schutz 1986; Holz & Hughes 2005; MacLeod & Hogan 2008; Nissanke et al. 2010, 2013; Del Pozzo 2012; Nishizawa 2017; Chen et al. 2018; Feeney et al. 2019; Mortlock et al. 2018; Vitale & Chen 2018). Chen et al. (2018) predicted that we will be able to constrain H_0 with 2% precision within 5 yr with standard sirens detected by the Laser Interferometer Gravitational-Wave Observatory (LIGO)/Virgo, while Nair et al. (2018) predicted a ∼7% measurement with just 25 binary–black-hole (BBH) events from the Einstein telescope.

Anticipating that the LIGO/Virgo Collaboration (LVC) network of GW detectors would eventually achieve sensitivity sufficient to enable standard siren-based measurements, the Dark Energy Survey (DES) collaboration and external collaborators launched in 2015 the DES gravitational waves (DESGW) program. DESGW uses the Dark Energy Camera (DECam) to search for optical emission associated with LVC-detected mergers and pursues cosmological measurements with standard sirens. In particular, the multi-messenger shared discovery of the neutron-star merger GW170817, and of its optical kilonova, resulted in a measurement of H_0 (Abbott et al. 2017a) that inaugurated the era of siren-based cosmology. We have also performed the most comprehensive searches for optical emission to black hole events, including GW150914 (Soares-Santos et al. 2016), GW151226 (Cowperthwaite et al. 2016), and GW170814 (Doctor et al. 2018). These events are expected to be dark, although the possibility of optical emission has yet to be observationally excluded.

Dark sirens can also be used for cosmology using a statistical method, as first proposed in Schutz (1986). Provided a catalog of potential host galaxies within the event localization region, their redshifts will contribute in a probabilistic way to the measurement of H_0, depending on the galaxies' distance and sky position. This approach has been developed within a Bayesian framework by Del Pozzo (2012) and Chen et al. (2018) and implemented in Fishbach et al. (2019) using GW170817, which produced results consistent with the first measurement (Abbott et al. 2017a) where the identified host galaxy, NGC 4993 (e.g., Palmese et al. 2017), was used. Eventually, a large sample of events will enable precise cosmological measurements using the dark siren approach.

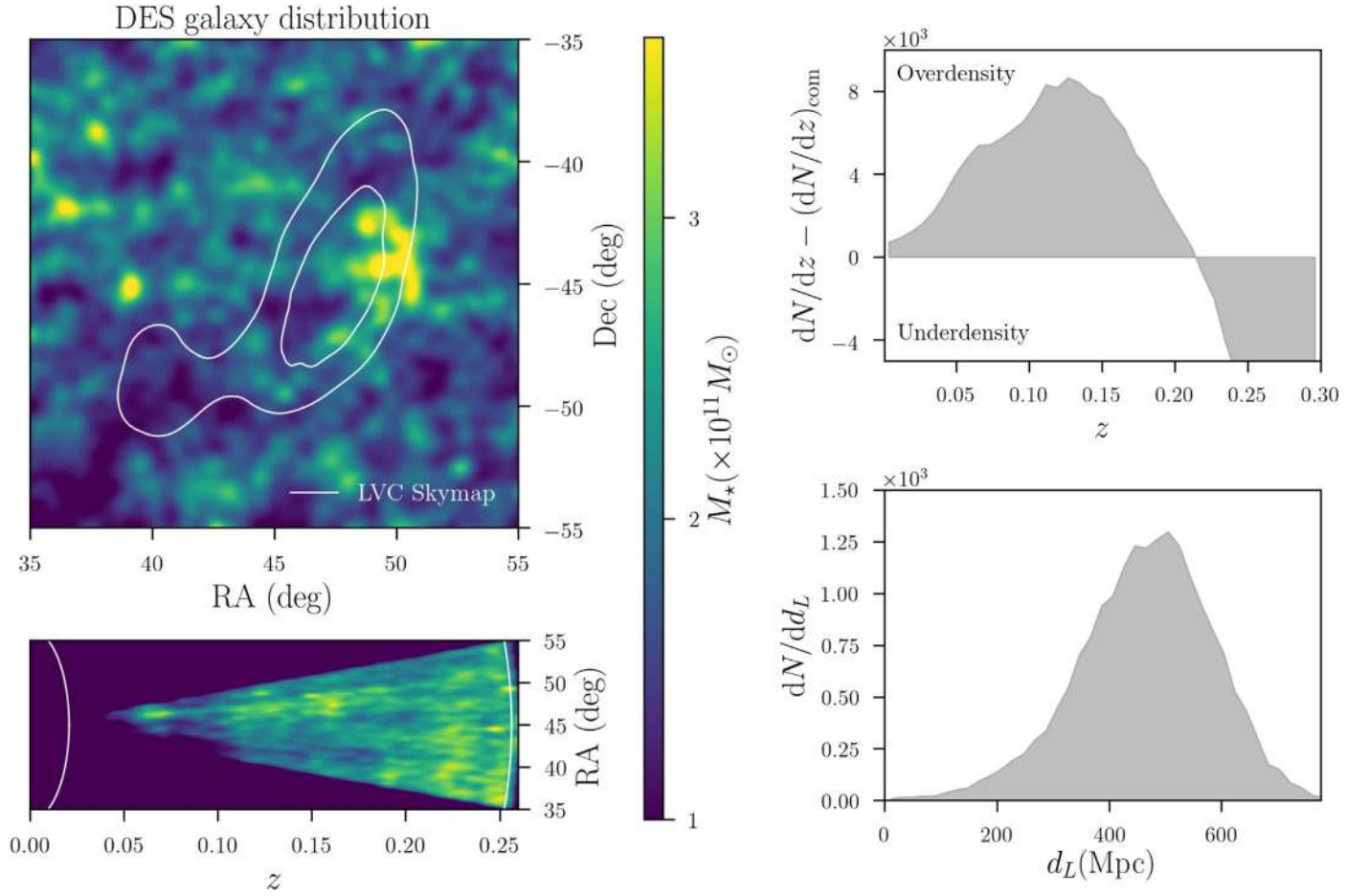

Figure 1. Left: stellar mass distribution of the DES galaxies used in this analysis (color map) and the GW170814 localization region at 50% and 90% CL (white contours). The region in redshift space is valid for the prior range $20 < H_0 < 140$ km s^{-1} Mpc^{-1}. The stellar mass map has been smoothed with a Gaussian filter of width 0°.3. The bottom panel shows the galaxies' stellar mass distribution in R.A. and redshift, projected over the decl. Right: distributions of the DES galaxy redshifts within the region of interest (top) and the luminosity distance in HEALPIX pixels from the LVC distance likelihood, as given in the sky map (bottom). The histograms are obtained from a Monte-Carlo (MC) sampling the galaxies' redshift probability distribution function (PDF) and the luminosity distance likelihood in each pixel. The redshift distribution has been subtracted by a uniform distribution in comoving volume $(dN/dz)_{\mathrm{com}}$, obtained assuming $H_0 = 70$ km s^{-1} Mpc^{-1}, and containing the same total number of galaxies to highlight the overdensity of galaxies in the region.

In this work, we measure H_0 using the GW event GW170814 (Abbott et al. 2017b) as a dark siren. GW170814 resulted from the inspiral and merger of a BBH system at a luminosity distance of 540^{+130}_{-210} Mpc (median value with 90% credible interval). The masses of the black holes were $30.5^{+5.7}_{-3.0}$ and $25.3^{+2.8}_{-4.2}\,M_\odot$, respectively. GW170814 is the first BBH detected by a triple network (including LIGO Hanford and Livingston, plus Virgo), and it has the smallest localization volume of any of the BBH events detected by LVC thus far. Therefore, the number of potential host galaxies is lower compared to other events, making GW170814 the most appropriate event for this measurement. Additionally, the event localization region falls within the DES footprint, making DES galaxy catalogs a prime sample for measurement of H_0. With this one event, our goal is to provide a proof of principle measurement, addressing the challenges that are specific to the dark siren method, and establishing its potential to yield precision cosmology results in the near future.

A key component of the measurement is crafting the appropriate galaxy catalog: completeness, as well as precise and accurate photometric redshifts (photo-z's), throughout the entire volume probed are required. The overlap of GW170814's area with DES allows us to employ galaxy catalogs produced from the first three years of the survey (DES Y3; Abbott et al. 2018). This first dark siren measurement is a step toward incorporating this new cosmological probe into the portfolio of cosmic surveys for dark energy.

A detailed description of the data used in this analysis is provided in Section 2, followed by a description of our implementation of the method in Section 3. We present our results and discussion in Section 4, and our conclusions in Section 5. Throughout this Letter we assume a flat ΛCDM cosmology with $\Omega_m = 0.3$ and H_0 values in the 20–140 km s^{-1} Mpc^{-1} range. All quoted error bars represent the 68% confidence level (CL), unless otherwise stated.

2. Data

2.1. The LVC Sky Map

The sky map used in this work is the publicly available `LALInference` map (LIGO Scientific Collaboration & Virgo Collaboration 2017),[230] provided in HEALPIX (Górski et al. 2005) pixels. The luminosity distance probability distribution is approximated with a Gaussian in each pixel.

[230] https://dcc.ligo.org/LIGO-T1700453/public

The region of interest, enclosing 90% of the localization probability, is 61.66 deg^2. The projected sky map and the distribution of luminosity distance mean values from the LVC distance likelihood in each pixel within the region of interest are shown in Figure 1. The probability peak is located at R.A., decl. = (47.°523, −44.°856). At the peak location, the luminosity distance is 504.7 Mpc and the Gaussian width is 91.9 Mpc. Using the limiting values of our H_0 prior range ([20,140] km s^{-1} Mpc^{-1}) we can convert the 90% and 99.7% distance range into a redshift range ($0.02 < z < 0.26$ and $z < 0.3$, respectively) for this analysis.

2.2. The DES Galaxy Catalog

The DES[231] (The Dark Energy Survey Collaboration 2005; Dark Energy Survey Collaboration et al. 2016) is an optical–near-infrared survey that images 5000 deg^2 of the South Galactic Cap in the *grizY* bands. The survey is being carried out using a ∼3 deg^2 charge-coupled device (CCD) camera (the DECam, see Flaugher et al. 2015) mounted on the Blanco 4 m telescope at the Cerro Tololo Inter-American Observatory (CTIO) in Chile. The data used here are from the first 3 yr of observations (2013 September–2016 February; Abbott et al. 2018).

The DES Data Management (DESDM) pipeline was used for data reduction (Morganson et al. 2018). The process includes calibration of the single-epoch images, which are co-added after background subtraction and then cut into tiles. The source catalog was created using SOURCE EXTRACTOR (SEXTRACTOR; Bertin & Arnouts 1996) to detect objects on the *riz* co-added images. The median 10σ limiting magnitudes of Y3 data for galaxies are $g = 24.33$, $r = 24.08$, $i = 23.44$, $z = 22.69$, and $Y = 21.44$ mag (Abbott et al. 2018). The photometry used in this work is part of a value-added Y3 catalog not released with the first data release (DR1), and is the result of the Multi-Object Fitting (MOF) pipeline that uses the `ngmix` code.[232] Following a procedure similar to Drlica-Wagner et al. (2017) for Year 1 data, the DES collaboration made further selections to produce a high-quality object catalog called the Y3 "gold" catalog. For this sample, redshifts have been computed using the Directional Neighborhood Fitting (DNF; De Vicente et al. 2016), and they are not included in DR1.

The DNF method applied to Y3 data provides redshift information for each galaxy in the form of a probability distribution function (PDF), from which a mean redshift, and half of the central 68th percentile width, are computed. The width of the PDF can be over or underestimated due to the sampling of the training set and algorithmic details of DNF. This issue is particularly relevant for the redshift range used in this work, which is low compared to that exploited in weak lensing and large-scale structure cosmology, for which the DNF method was optimized. We find that the typical uncertainty below redshift $z \sim 0.1$ is underestimated by a factor of 10 when compared to the typical scatter found for the subset of the galaxies with available spectroscopic redshifts (where the standard deviation is $\sigma \gtrsim 0.015$). Thus, we add a minimum uncertainty of 0.015 for these low-z galaxies. At $0.1 < z < 0.3$, the uncertainty is well behaved and the average value follows $\bar{\sigma}_z(z) \simeq 0.013\ (1+z)^3$, as we find using an empirical fit.

We produce alternative photo-z estimates with another machine-learning code, ANNZ2 (Sadeh et al. 2016). This allows us to test the impact of the correction applied to the DNF errors on the posterior of the Hubble constant. Photo-z with ANNZ2 have previously been validated for cosmological analyses using DES Science Verification data (Abbott et al. 2016; Bonnett et al. 2016; Leistedt et al. 2016) and for the Kilo-Degree Survey (KiDS; Bilicki et al. 2018), and are produced as part of the DES photo-z pipeline (Gschwend et al. 2018). In particular, it provides error estimates through a k-nearest neighbor (kNN) method, and dedicated redshifts for the purposes of this analysis. We additionally employ a reweighting technique (Lima et al. 2008) specifically for our galaxy sample to further tune our redshifts. We run ANNZ2 in randomized regression mode with 50 Boosted Decision Trees, using a spectroscopic sample of 245,458 matching Y3 galaxies out to redshift $z \gtrsim 1$, randomly split into subsamples for training, testing, and validation. The training and the reweighting use *griz* MOF magnitudes. We find that the typical error roughly follows $\sim 0.02\ (1+z)^3$ in the redshift range of interest. The two algorithms, DNF and ANNz2, gave similar results; see Section 4.

These redshifts, together with publicly available spectroscopic redshifts from 2dF, 6dF, and SPT-GMOS (Colless et al. 2001; Jones et al. 2009; Bayliss et al. 2016) and the DES MOF photometry, are used to estimate galaxy properties (including stellar mass and absolute magnitude) of this sample. This is achieved through a broadband spectral energy distribution (SED) fitting of galaxy magnitudes with LEPHARE (Arnouts et al. 1999, Ilbert et al. 2006). Estimates of the galaxy properties used here from DES data alone have been tested and studied in several DES works (Palmese et al. 2016; Etherington et al. 2017; Palmese et al. 2019). We add a 0.05 systematic uncertainty in quadrature to the magnitudes, to account for systematic uncertainties in magnitude estimation and model variance.[233] The simple stellar population templates used for the fitting are Bruzual & Charlot (2003), with three metallicities ($0.2\,Z_\odot$, $Z_\odot$ and $2.5\,Z_\odot$), a Chabrier (2003) initial mass function and a Milky Way (Allen 1976) extinction law with five different values between 0 and 0.5 for the $E(B-V)$ reddening. The star formation history chosen is exponentially declining as $e^{-t/\tau}$ with $\tau = 0.1$, 0.3, 1, 2, 3, 5, 10, 15, and 30 Gyr.

The source list of the Y3 gold catalog is 95% complete for galaxies within our apparent magnitude limit, $r < 23.35$ (Abbott et al. 2018). This value is computed through the recovery rate of sources from the deeper Canada-France-Hawaii Telescope Lensing Survey (CFHTLenS; Erben et al. 2013), and thus includes the correct distribution of surface brightnesses. Nevertheless, extended, low surface brightness galaxies near our flux limit may be preferentially missed by the detection pipeline. We therefore provide an approximate completeness of sources throughout the redshift range of interest. Using DNF mean redshifts, we convert the source completeness to $r < 23.35$ from Abbott et al. (2018, their Figure 12) into a completeness in redshift intervals, $\Delta z = 0.02$. By taking the peak of the magnitude distribution in each bin as roughly our observed magnitude limit at that redshift, we find our sample is >93% complete across the range $0 < z < 0.26$. We further determined that the fraction of low-redshift,

[231] www.darkenergysurvey.org
[232] https://github.com/esheldon/ngmix
[233] This is a regularization to compensate for the synthetic model set grid and the fact that many SED fitting codes do not include a model error function. The value chosen is based on past experience of what gives stable results.

extended galaxies missed by the DES Y3 pipeline is ∼1%, when compared with the Two Micron All-Sky Survey (2MASS) extended source catalog (Huchra et al. 2012). For the purpose of this Letter, we choose to ignore those ultra-low-z sources as most of them are at $z < 0.02$ and are not relevant for the present analysis.

The DES Y3 gold catalog, is nonetheless, an observed magnitude-limited sample. This analysis requires a volume-limited sample, which we obtain by applying a luminosity cut. In order to determine the appropriate cut to create a volume-limited sample, we compute the completeness limits in terms of absolute quantities (luminosity and stellar mass). We follow the method outlined in Pozzetti et al. (2010) and Hartley et al. (2013). We identify galaxies with observed magnitudes that are bright enough to be complete and representative of the real galaxy population within redshift bins. To compute the 95% completeness limit in (rest-frame) luminosity, we scale the luminosities of this sample to that which they would have if their observed magnitude were equal to the survey completeness limit, and take the 95th percentile of the resulting luminosity distribution. This value corresponds to -17.2 in r-band absolute magnitude and $\sim 3.8 \times 10^8\ M_\odot$ in stellar mass for the redshift range of interest. We cut the DES catalog at the specific absolute luminosity value mentioned above. We conclude that our volume-limited galaxy sample is complete within the redshift range of interest for galaxies down to stellar masses of $\sim 3.8 \times 10^8\ M_\odot$. In other words, our galaxy catalog contains ∼77% of the total stellar mass in the volume considered by assuming that the galaxies follow a Schechter stellar mass function with the best-fit values from Weigel et al. (2016).

The final galaxy stellar mass and redshift distributions of galaxies are shown in Figure 1. The stellar mass map clearly shows the presence of large-scale structure, including clusters, voids, and filaments. We recognize a number of well-known clusters within the volume of interest, including several Abell clusters. A uniform distribution of galaxies in comoving volume $(dN/dz)_{\rm com}$ has been subtracted from the observed galaxies' redshift distribution in Figure 1 to highlight the overdensities. The $(dN/dz)_{\rm com}$ distribution has been obtained by assuming $H_0 = 70$ km s^{-1} Mpc^{-1} and it contains the same total number of galaxies as the observed dN/dz over the redshift range shown. We are able to identify a "wall"-like structure around $z \sim 0.06$ spanning most of the area between $35 <$ R.A. < 55 and $-55 <$ decl. < -35, which is spectroscopically confirmed by 2dF, LCRS, (Shectman et al. 1996), and especially 6dF. A broader galaxy overdensity is found around $z \sim 0.12$ (also seen in LCRS and 2dF, and composed of several Abell galaxy clusters). This broad peak is also identified in redshift distributions by other photo-z codes, including a template-based code, the Bayesian Photometric Redshift (Benéz 2000). We have further verified that overdensities at the lowest redshifts ($z \sim 0.06$) are also present in spectroscopic samples outside of the region of interest. This is expected at these low redshifts, where large-scale structure projects onto vast areas of the sky. In summary, there are 77,092 galaxies within the 90% LIGO/Virgo probability volume, and 105,011 when 99.7% of the distance probability is considered, of which ∼6000 have spectroscopic redshifts.

3. Method

In order to estimate the posterior probability of H_0 given GW data $d_{\rm GW}$ from a single event detection, and electromagnetic (EM) data from a galaxy survey, we follow Chen et al. (2018). By applying Bayes' theorem, one can write the posterior as

$$p(H_0|d_{\rm GW}, d_{\rm EM}) \propto p(d_{\rm GW}, d_{\rm EM}|H_0)p(H_0). \quad (1)$$

We assume that all cosmological parameters except for H_0 are fixed (flat ΛCDM cosmology with $\Omega_m = 0.3$ and $\Omega_\Lambda = 0.7$). We treat the joint GW and EM likelihood $p(d_{\rm GW}, d_{\rm EM}|H_0)$ as the product of two individual likelihoods (as the processes involved in producing the data from the two experiments are independent) marginalized over all variables except for the true luminosity distance d_L and solid angle $\hat{\Omega}_{\rm GW}$ of the GW source, and for the true host galaxy redshift z_i and solid angle $\hat{\Omega}_i$. Note that the solid angles $\hat{\Omega}$ are vectors with the angular position of the source/galaxy as direction, and they all subtend the same area ($\sim 3 \times 10^{-3}$ deg^2) as the sky is pixelized with HEALPIX maps in this work. If we assume that the event happened in one of the observed galaxies i, then $\hat{\Omega}_{\rm GW}$ and $\hat{\Omega}_i$ are related, and so are d_L and z_i through the cosmology (in this case, H_0). By marginalizing also over the choice of galaxy i, the joint marginal likelihood can be written as

$$\begin{aligned} &p(d_{\rm GW}, d_{\rm EM}|\{z_j, \hat{\Omega}_j\}, H_0) \\ &\quad \propto \textstyle\sum_i w_i \int dd_L\, d\hat{\Omega}_{\rm GW}\, p(d_{\rm GW}|d_L, \hat{\Omega}_{\rm GW}) \\ &\quad \times p(d_{\rm EM}|\{z_j, \hat{\Omega}_j\})\delta_D(d_L - d_L(z_i, H_0))\delta_D(\hat{\Omega}_{\rm GW} - \hat{\Omega}_i), \end{aligned} \quad (2)$$

where δ_D is the Dirac delta function, w_i are weights that represent the relative probability that different galaxies host a GW source, and $\{z_j, \hat{\Omega}_j\}$ represents all the galaxies' redshift and solid angle. These weights could be based on some galaxy properties, such as luminosity or star formation rate, but here we assume they are uniform across all galaxies given our lack of knowledge of GW host galaxy properties.

We also need to marginalize over the galaxies' redshifts and sky positions, with a reasonable choice of prior $p(z_i, \Omega_i)$. If one assumes that the galaxies are uniformly distributed in comoving volume V, and volume-limited within $V_{\rm max}$,

$$p(z_i, \hat{\Omega}_i)\, dz_i\, d\hat{\Omega}_i \propto \frac{1}{V_{\rm max}} \frac{d^2V}{dz_i d\hat{\Omega}_i} dz_i\, d\hat{\Omega}_i \propto \frac{1}{V_{\rm max}} \frac{r^2(z_i)}{H(z_i)} dz_i\, d\hat{\Omega} \quad (3)$$

where r is the comoving distance to the galaxy. While this assumption holds on average over sufficiently large volumes, it is possible that future precision cosmology analyses will require taking into account the real clustering of galaxies in this formalism.

Assuming that we precisely know the galaxies' positions $\{\hat{\Omega}_j\}$ (which is realistic especially in the limit in which spatial probabilities are considered within HEALPIX pixels), we can integrate over the galaxies' positions as delta functions about the observed values. The marginal EM likelihood reduces to $p(d_{\rm EM}|\{z_j\})$, which we approximate for simplicity by a product of Gaussian distributions, $\mathcal{N}$, for each galaxy, centered around the observed redshift values $z_{{\rm obs},i}$ with a width given by the

redshift's uncertainty $\sigma_{z,i}$ for each galaxy i:

$$p(d_{\rm EM}|\{z_j\}) = \prod_i p(z_{{\rm obs},i}|z_i) = \prod_i \mathcal{N}(z_{{\rm obs},i}, \sigma_{z,i}; z_i). \quad (4)$$

The marginal GW likelihood $p(d_{\rm GW}|d_L, \Omega)$ can be computed as prescribed in Singer et al. (2016):

$$p(d_{\rm GW}|d_L, \hat{\Omega}) \propto p(\hat{\Omega}) \frac{1}{\sqrt{2\pi}\sigma(\hat{\Omega})} \exp\left[-\frac{(d_L - \mu(\hat{\Omega}))^2}{2\sigma^2(\hat{\Omega})}\right] N(\hat{\Omega}), \quad (5)$$

where the position probability, location, normalization, and scale (PROB $p(\hat{\Omega})$, DISTMU μ, DISTNORM N, and DISTSTD σ, respectively) of the luminosity distance at each position are provided in the sky map.

We now consider the selection effects of GW events and galaxies introduced by the experiments' sensitivities and detection pipelines. We follow the approach of Chen et al. (2018) and Mandel et al. (2019), and include a $[\beta(H_0)]^{-1}$ factor that normalizes the likelihood over all possible GW and EM data. Given that our galaxy catalog is volume-limited out to larger distances than the maximum observable distance for the GW events, this term reduces to

$$\beta(H_0) = \frac{V[d^{\rm max}_{L,{\rm GW}}(H_0)]}{V_{\rm max}(H_0)}, \quad (6)$$

where $V[d^{\rm max}_{L,{\rm GW}}(H_0)]$ is the maximum observable volume for the GW events considered.

Finally, Equation (1) becomes

$$p(H_0|d_{\rm GW}, d_{\rm EM}) \propto \frac{p(H_0)}{V[d^{\rm max}_{L,{\rm GW}}(H_0)]} \sum_i \frac{1}{\mathcal{Z}_i} \times \int dz_i\, p(d_{\rm GW}|d_L(z_i, H_0), \hat{\Omega}_i) p(d_{\rm EM}|z_i) \frac{r^2(z_i)}{H(z_i)}, \quad (7)$$

where $\mathcal{Z}_i = \int p(d_{\rm EM}|z_i) r^2(z_i) / H(z_i)\, dz_i$ are evidence terms that arise from integrating out the other galaxy redshifts in each term of the sum. This formalism can be extended to combine data $\{d_{{\rm GW},j}\}$ and $d_{\rm EM}$ from a sample of multiple events j, assuming that the GW events are independent and that the galaxy catalog is fixed for all events:

$$p(H_0|\{d_{{\rm GW},j}\}, d_{\rm EM}) \propto p(H_0) \int d^N z_k d^N \hat{\Omega}_k p(z_k, \hat{\Omega}_k) \times p(d_{EM}|\{z_k, \hat{\Omega}_k\}) \left[\prod_j p(d_{GW,j}|\{z_k, \hat{\Omega}_k\})\right]. \quad (8)$$

In the following, we assume a flat prior on H_0 within [20,140] km s^{-1} Mpc^{-1}, unless otherwise stated. This is a very broad prior, covering a range that is much larger than current estimates of H_0. This choice was made as a compromise between the following aspects: (i) a result that is mostly informed by the LVC and DES data rather than by external constraints, (ii) a result that can be compared with the first standard siren estimate, and (iii) a complete galaxy sample that contains most of the stellar mass within the localization volume, to minimize the chance of missing the real host galaxy. As explained in more detail in Section 4, the redshift cut is related to the H_0 prior range, and in order to explore higher values of H_0, one needs to include higher redshift galaxies, and make a higher luminosity cut to preserve the volume-limited sample.

A blinded analysis has been performed when estimating the H_0 posterior from the data to avoid confirmation bias. The values of the Hubble constant have been randomly displaced by an unknown amount, and we unblinded after our pipeline was able to reliably reproduce the input cosmology on simulation tests.

4. Results and Discussion

We apply the described methodology to the DES galaxies' redshifts and the GW170814 LIGO/Virgo sky map to produce a posterior distribution for the Hubble constant. We find that changes in the H_0 estimate and its uncertainty between using the corrected DNF photo-z's or the ANNZ2 outputs are below the percent level. This agreement is expected, because the two methods produce redshift distributions that are consistent with similar uncertainties. We also add a 0.001 systematic redshift error in quadrature (corresponding to a typical peculiar velocity of $\sim$300 km s^{-1}). The effect of this correction on the posterior is negligible because only a few percent of the galaxies have a spectroscopic redshift, and the effect of peculiar velocities on the remaining galaxies is more than an order of magnitude below their typical photo-z error.

Our maximum a posteriori estimate of the Hubble constant is $H_0 = 75^{+40}_{-32}$ km s^{-1} Mpc^{-1} using a flat prior between 20 and 140 km s^{-1} Mpc^{-1}. The full posterior distribution is shown in Figure 2, and Table 1 summarizes our findings. The presence of a main, though broad, peak, is expected given the large-scale structure seen in the observed volume.

As described in Section 2.1, the galaxy sample used in these results is selected as described in Section 2, and covers the LIGO/Virgo 90% credible localization volume. The distance cut is translated into a redshift cut (made on the mean photo-z value of each galaxy) for a given H_0 prior. This cut ensures that the galaxy catalog is as complete as possible throughout the whole redshift range of interest for the cosmological parameters used, and includes the fainter galaxies observable for a volume-limited sample defined as in Section 2. In fact, in order to include more distant galaxies, the luminosity cut needs to be brighter to ensure that the sample is still volume limited, with the risk of missing the true host galaxy. We have explored the impact of the redshift cut on the H_0 posterior, while keeping the angular selection to be within the 90% credible localization area. The effect of including galaxies out to 99.7% of the distance localization (corresponding to $z \lesssim 0.3$) is most pronounced at high H_0 values, as shown by the shaded red region in Figure 2. With this less restrictive cut, the credible region shifts to $H_0 = 77^{+41}_{-33}$ km s^{-1} Mpc^{-1}, showing a $\sim$2% change of the maximum. The effect described here arises from tens of thousand of galaxies at the higher redshifts included with the more relaxed distance cut and the ansatz of Gaussianity of the luminosity distance posterior. In fact, these galaxies contribute with a non-negligible probability to the posterior because of the high d_L tail shown in the bottom-right panel of Figure 1, and they contribute more significantly at high H_0 values. This few percent effect is insignificant at the current levels of precision, but will need to be explored in the future using a more realistic luminosity distance posterior.

Our result agrees well (as expected, due to the large uncertainty) with the latest CMB estimate of the Hubble constant by the *Planck* Collaboration (67.36 ± 0.54 km s^{-1} Mpc^{-1} from TT,TE,EE+lowP+lensing; Planck Collaboration et al. 2018), and with results using distance ladder methods by ShoES

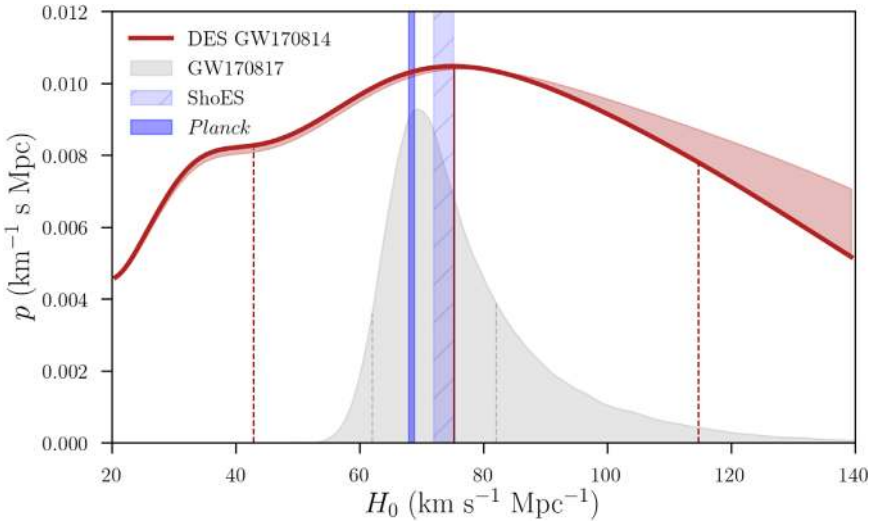

Figure 2. Hubble constant posterior distribution obtained by marginalizing over ~77,000 possible host galaxies (red line), showing the maximum value (solid vertical line). The maximum a posteriori and its 68% confidence level is $H_0 = 75^{+40}_{-32}$ km s^{-1} Mpc^{-1} for a flat prior in the range [20,140] km s^{-1} Mpc^{-1}. The shaded region represents the change in the posterior when different fractions of the localization volume are considered (from 90% to 99.7% of the LIGO/Virgo luminosity distance posterior). The PDF computed from the larger volume has been renormalized to have the same value of the 90% localization volume H_0 posterior at the maximum, to highlight differences below and beyond the main peak. The posterior obtained by Abbott et al. (2017a) for the bright standard siren event GW170817, associated to one galaxy, is shown in gray. The prior used in that work was flat-in-log over a narrower range ([50,140] km s^{-1} Mpc^{-1}), and the posterior has been rescaled by a factor 0.2 for visualization purposes. The 68% CL of both PDFs is shown by the dashed lines. Constraints from *Planck* (Planck Collaboration et al. 2018) and Supernovae and H_0 for the Equation of State (SHoES; Riess et al. 2016, 2018) at 1σ are shown in purple boxes.

Table 1
Hubble Constant Estimate from this Work

Prior	H_0	$+\sigma_{H_0}$	$-\sigma_{H_0}$	σ_{H_0}/H_0	σ_{H_0}/H_0 prior
[20,140]	75	40	32	47.8%	54.3%

Note. All H_0 values and errors are in km s^{-1} Mpc^{-1}. The uncertainty from the flat prior only is derived by assuming the same H_0 maximum found in the analysis. Quoted uncertainties represent 68% confidence level around the maximum of the posterior, and they are statistical only. The last column quantity (σ_{H_0}/H_0 prior) corresponds to 68% times the prior width divided by H_0.

(73.52 ± 1.62 km s^{-1} Mpc^{-1}; Riess et al. 2016) and by DES (67.77 ± 1.30 km s^{-1} Mpc^{-1} from SN+BAO; Macaulay et al. 2019).

For the bright standard siren measurement using GW170817 and its electromagnetic counterpart, Abbott et al. (2017a) found $H_0 = 70.0^{+12.0}_{-8.0}$ km s^{-1} Mpc^{-1} at 68% credible interval. Without an EM counterpart leading to a unique host galaxy redshift, we would have recovered a broader H_0 posterior because we average over all possible host galaxies in the localization volume. For example, Fishbach et al. (2019) applied the statistical standard siren method to GW170817 and found a larger uncertainty than the counterpart standard siren result: $H_0 = 76^{+48}_{-23}$ km s^{-1} Mpc^{-1} for a uniform prior over the range [10,220] km s^{-1} Mpc^{-1}. For a BBH standard siren measurement, as in this work, the combination of the larger localization volume (implying a significantly greater number of potential host galaxies) and the large photometric redshift uncertainty for each galaxy results in an even broader H_0 posterior. Therefore, while applying the statistical standard siren method to GW170817 yields a 68% credible region on H_0 comprising 34% of the prior range (Fishbach et al. 2019), in this work we obtain a 68% credible region on H_0 that is 60% of the prior range. We note that the prior used in Fishbach et al. (2018) is 1.75 times broader than the prior used in this work; if we adopt the same broader prior of [10,220] for our analysis of GW170814, we find $H_0 = 78^{+96}_{-24}$ km s^{-1} Mpc^{-1}. The dependence of the width of the H_0 posterior on the prior width is a consequence of the fact that the GW observation, which provides only a luminosity distance estimate, is consistent with arbitrarily large H_0's, if there are galaxies at sufficiently large redshifts. If the galaxy catalog extends to some redshift, $z_{\rm max}$, the posterior would fall off around $H_0 \approx cz_{\rm max}/d_L$, where d_L is the typical luminosity distance from the GW posterior. However, this fall off is artificial as there are galaxies at greater redshifts that are not included in the catalog. These may be accounted for using catalog incompleteness corrections. We chose the prior range for this analysis rather than a larger one such that we did not need to include such corrections, which simplifies the analysis. However, dark siren measurements will become particularly interesting when multiple events can be combined and this effect becomes irrelevant (Chen et al. 2018).

The analysis in Fishbach et al. (2019) for GW170817 used the Galaxy List for the Advanced Detector Era (GLADE) galaxy catalog (Dálya et al. 2018), and accounted for incompleteness at the distance of GW170817. GLADE becomes significantly incomplete at the distance to GW170814. As GW detectors improve in sensitivity, the majority of dark standard sirens will be detected at even greater distances and with larger localization volumes, well beyond the reach of spectroscopic galaxy catalogs. This highlights the need for reliable and complete photometric galaxy catalogs. Surveys such as DES, Pan-STARRS1 (Chambers et al. 2016), and the Large Synoptic Survey Telescope (LSST) are therefore likely to play an important role in future constraints from BBH standard sirens.

The assumption throughout this work is that even if the event occurred in a galaxy below our luminosity threshold, large-scale structure predicts that fainter galaxies follow the clustering pattern of the more luminous galaxies in our sample. We have verified in our simulations that a threshold up to 1 mag brighter than the limit used here to place events has a

negligible impact over a sample of 100 events, provided that the catalog is volume limited for the range of redshifts relevant to the measurement.

Galaxies are biased tracers of the universe's dark matter, therefore some theories predict that the origin of the black holes involved in these GW events is primordial, constituting part or all of the dark matter (Bird et al. 2016; Clesse & García-Bellido 2017, 2018; García-Bellido 2017). In that case, GW events follow exactly the underlying dark matter distribution (presenting an unbiased tracer). Because of the stellar mass to dark matter halo connection (see Wechsler & Tinker 2018, and references therein) it is reasonable to weight galaxies by their stellar mass in Equation (2) as $w_i \propto M_\star$. The impact of this scaling with stellar mass or star formation rate has been explored in Fishbach et al. (2019). We find that the stellar mass weighting has a negligible effect on the posterior. This is due to the large volume analyzed (over which the stellar masses tend to be averaged out) and to the precision level of this measurement. In other theories, these black hole binaries are produced in very-low-metallicity galaxies (e.g., Cao et al. 2018; Mapelli et al. 2018), biased relative to the dark matter distribution differently than the luminous galaxies in our catalog. J. Annis et al. (2019, in preparation) explore the effect of the tracer bias assumptions on the H_0 posterior for future analyses aiming at precision measurements.

Another assumption of our analysis that needs attention concerns the redshift likelihood. As anticipated above for the GW likelihood, this will not, in general, be well approximated by a Gaussian. In the future, we plan to explore the impact of realistic photometric redshift PDFs on the H_0 posterior, in order to enable precision cosmology with BBH events. An analysis with the full, asymmetric, GW likelihood will also be required. While an estimate of those effects is needed, tests on off-source lines of sight show that our constraint is likely not strongly impacted by the photo-z training sample or systematic failures.

In the past two LVC observing seasons, black hole mergers outnumbered neutron star events at a rate of approximately 10–1. Uncertainties on the expected detection rate are large, but conservative estimates predict $\sim$1 event per week for the upcoming observing campaign (scheduled to start in 2019 April). The majority of these events will have larger localization volumes than GW170814 (Chen & Holz 2016 estimated that $\lesssim$1% of BBHs will be localized to better than 10^4 Mpc^3), and hence provide poorer constraints than those reported here. However, given the high expected event rate for dark sirens, larger event samples will be available in the future. Chen et al. (2018) provided forecasts using a distribution of realistic localization area, finding that the dark siren method will reach $\sim$10% statistical precision on H_0 by 2026 from BBH mergers only, and 5%–10% precision from BNS mergers if none of them have EM counterparts.

5. Conclusions

In this Letter, we have performed the first measurement of the Hubble constant using a GW detection of a BBH merger as a dark standard siren and the DES galaxies as a sample of potential host galaxies. Our analysis was blinded to avoid confirmation bias. Our main results, discussed in Section 4, include a measurement of $H_0 = 75^{+40}_{-32}$ km s^{-1} Mpc^{-1} for a flat prior within [20,140] km s^{-1} Mpc^{-1}, which is consistent with previous measurements of H_0. The 68% confidence interval quoted here is 60% of the uniform prior range, and it depends on the width of the prior. For example, with a broader prior of [10,220] km s^{-1} Mpc^{-1}, we find $H_0 = 78^{+96}_{-24}$ km s^{-1} Mpc^{-1}. Albeit weak, this measurement is not uninformative and the method becomes more powerful when we combine large numbers of dark sirens (Chen et al. 2018).

Future dark siren measurements will require complete galaxy catalogs. A wide field galaxy catalog with a DES-like depth is currently available only for $\sim$one-eighth of the sky. However, DES can be complemented with other data sets taken with DECam (such as the Blanco Imaging of the Southern Sky, BLISS, and the Dark Energy Camera Legacy Survey (DECals)), to cover the whole Southern sky to a good depth ($r \sim 23.4$, 5σ depth). An even deeper survey with more precise photo-z's, such as the LSST (LSST Dark Energy Science Collaboration 2012), would be of great value for further improving these constraints.

At the expected level of precision from hundreds of events ($<$10%), systematics will play an important role. In future work, we plan to incorporate systematic uncertainties in our simulated data studies, in order to prepare for precision cosmology analyses on real data. We anticipate that some of the main sources of systematics will be photo-z biases and catastrophic outliers, photo-z training sample sample variance, galaxy catalog cuts, and galaxy catalog completeness. In order to achieve the full potential of statistical standard siren cosmology, wide and deep galaxy surveys such as DES and LSST are necessary. Overall, our findings show that the synergy between GW black hole merger detections and new-generation large galaxy surveys will establish a new powerful probe for precision cosmology.

Funding for the DES Projects has been provided by the DOE and NSF (USA), MEC/MICINN/MINECO (Spain), STFC (UK), HEFCE (UK). NCSA (UIUC), KICP (University of Chicago), CCAPP (Ohio State), MIFPA (Texas A&M), CNPQ, FAPERJ, FINEP (Brazil), DFG (Germany), and the Collaborating Institutions in the Dark Energy Survey.

The Collaborating Institutions are Argonne Lab, UC Santa Cruz, University of Cambridge, CIEMAT-Madrid, University of Chicago, University College London, DES-Brazil Consortium, University of Edinburgh, ETH Zürich, Fermilab, University of Illinois, *ICE* (IEEC-CSIC), IFAE Barcelona, Lawrence Berkeley Lab, LMU München, and the associated Excellence Cluster Universe, University of Michigan, NOAO, University of Nottingham, Ohio State University, University of Pennsylvania, University of Portsmouth, SLAC National Lab, Stanford University, University of Sussex, Texas A&M University, and the OzDES Membership Consortium.

Based in part on observations at Cerro Tololo Inter-American Observatory, National Optical Astronomy Observatory, which is operated by the Association of Universities for Research in Astronomy (AURA) under a cooperative agreement with the National Science Foundation.

The DES Data Management System is supported by the NSF under grant Nos. AST-1138766 and AST-1536171. The DES participants from Spanish institutions are partially supported by MINECO under grants AYA2015-71825, ESP2015-88861, FPA2015-68048, and Centro de Excelencia SEV-2016-0588, SEV-2016-0597, and MDM-2015-0509. Research leading to these results has received funding from the ERC under the EU's 7th

Framework Programme including grants ERC 240672, 291329 and 306478. We acknowledge support from the Australian Research Council Centre of Excellence for All-sky Astrophysics (CAASTRO), through project number CE110001020.

This manuscript has been authored by Fermi Research Alliance, LLC under Contract No. DE-AC02-07CH11359 with the U.S. Department of Energy, Office of Science, Office of High Energy Physics.

The authors gratefully acknowledge the support of the United States National Science Foundation (NSF) for the construction and operation of the LIGO Laboratory and Advanced LIGO as well as the Science and Technology Facilities Council (STFC) of the United Kingdom, the Max-Planck-Society (MPS), and the State of Niedersachsen/Germany for support of the construction of Advanced LIGO and construction and operation of the GEO600 detector. Additional support for Advanced LIGO was provided by the Australian Research Council. The authors gratefully acknowledge the Italian Istituto Nazionale di Fisica Nucleare (INFN), the French Centre National de la Recherche Scientifique (CNRS), and the Foundation for Fundamental Research on Matter supported by the Netherlands Organisation for Scientific Research, for the construction and operation of the Virgo detector and the creation and support of the EGO consortium. The authors also gratefully acknowledge research support from these agencies as well as by the Council of Scientific and Industrial Research of India, the Department of Science and Technology, India, the Science & Engineering Research Board (SERB), India, the Ministry of Human Resource Development, India, the Spanish Agencia Estatal de Investigación, the Vicepresidència i Conselleria d'Innovació Recerca i Turisme and the Conselleria d'Educació i Universitat del Govern de les Illes Balears, the Conselleria d'Educació Investigació Cultura i Esport de la Generalitat Valenciana, the National Science Centre of Poland, the Swiss National Science Foundation (SNSF), the Russian Foundation for Basic Research, the Russian Science Foundation, the European Commission, the European Regional Development Funds (ERDF), the Royal Society, the Scottish Funding Council, the Scottish Universities Physics Alliance, the Hungarian Scientific Research Fund (OTKA), the Lyon Institute of Origins (LIO), the Paris Île-de-France Region, the National Research, Development and Innovation Office Hungary (NKFIH), the National Research Foundation of Korea, Industry Canada and the Province of Ontario through the Ministry of Economic Development and Innovation, the Natural Science and Engineering Research Council Canada, the Canadian Institute for Advanced Research, the Brazilian Ministry of Science, Technology, Innovations, and Communications, the International Center for Theoretical Physics South American Institute for Fundamental Research (ICTP-SAIFR), the Research Grants Council of Hong Kong, the National Natural Science Foundation of China (NSFC), the Leverhulme Trust, the Research Corporation, the Ministry of Science and Technology (MOST), Taiwan, and the Kavli Foundation. The authors gratefully acknowledge the support of the NSF, STFC, MPS, INFN, CNRS, and the State of Niedersachsen/Germany for provision of computational resources.

ORCID iDs

M. Soares-Santos https://orcid.org/0000-0001-6082-8529
A. Palmese https://orcid.org/0000-0002-6011-0530

References

Abbott, B. P., Abbott, R., Abbott, T. D., et al. 2016, PhRvL, 116, 061102
Abbott, B. P., Abbott, R., Abbott, T. D., et al. 2017, PhRvL, 119, 161101
Abbott, B. P., Abbott, R., Abbott, T. D., et al. 2017a, Natur, 551, 85
Abbott, B. P., Abbott, R., Abbott, T. D., et al. 2017b, PhRvL, 119, 141101
Abbott, T., Abdalla, F. B., Allam, S., et al. 2016, PhRvD, 94, 022001
Abbott, T. M. C., Abdalla, F. B., Allam, S., et al. 2018, arXiv:1801.03181
Allen, D. A. 1976, MNRAS, 174, 29P
Arcavi, I., Hosseinzadeh, G., Howell, D. A., et al. 2017, Natur, 551, 64
Arnouts, S., Cristiani, S., Moscardini, L., et al. 1999, MNRAS, 310, 540
Bayliss, M. B., Ruel, J., Stubbs, C. W., et al. 2016, ApJS, 227, 3
Benéz, N. 2000, ApJ, 536, 571
Bertin, E., & Arnouts, S. 1996, A&AS, 117, 393
Bilicki, M., Hoekstra, H., Brown, M. J. I., et al. 2018, A&A, 616, A69
Bird, S., Cholis, I., Muñoz, J. B., et al. 2016, PhRvL, 116, 201301
Bonnett, C., Troxel, M. A., Hartley, W., et al. 2016, PhRvD, 94, 042005
Bruzual, G., & Charlot, S. 2003, MNRAS, 344, 1000
Cao, L., Lu, Y., & Zhao, Y. 2018, MNRAS, 474, 4997
Chabrier, G. 2003, PASP, 115, 763
Chambers, K. C., Magnier, E. A., Metcalfe, N., et al. 2016, arXiv:1612.05560
Chen, H.-Y., Fishbach, M., & Holz, D. E. 2018, Natur, 562, 545
Chen, H.-Y., & Holz, D. E. 2016, arXiv:1612.01471
Clesse, S., & García-Bellido, J. 2017, PDU, 15, 142
Clesse, S., & García-Bellido, J. 2018, PDU, 22, 137
Colless, M., Dalton, G., Maddox, S., et al. 2001, MNRAS, 328, 1039
Coulter, D. A., Foley, R. J., Kilpatrick, C. D., et al. 2017, Sci, 358, 1556
Cowperthwaite, P. S., Berger, E., Soares-Santos, M., et al. 2016, ApJL, 826, L29
Dálya, G., Galgóczi, G., Dobos, L., et al. 2018, MNRAS, 479, 2374
Dark Energy Survey Collaboration, Abbott, T., Abdalla, F. B., et al. 2016, MNRAS, 460, 1270
Del Pozzo, W. 2012, PhRvD, 86, 043011
De Vicente, J., Sánchez, E., & Sevilla-Noarbe, I. 2016, MNRAS, 459, 3078
Doctor, Z., Kessler, R., Herner, K., et al. 2018, arXiv:1812.01579
Drlica-Wagner, A., Sevilla-Noarbe, I., Rykoff, E. S., et al. 2017, PhRvD, submitted
Erben, T., Hildebrandt, H., Miller, L., et al. 2013, MNRAS, 433, 2545
Etherington, J., Thomas, D., Maraston, C., et al. 2017, MNRAS, 466, 228
Feeney, S. M., Peiris, H. V., Williamson, A. R., et al. 2019, PhRvL, 122, 061105
Fishbach, M., Gray, R., Magaña Hernandez, I., et al. 2019, ApJL, 871, L13
Flaugher, B., Diehl, H. T., Honscheid, K., et al. 2015, AJ, 150, 150
Freedman, W. L. 2017, NatAs, 1, 0169
García-Bellido, J. 2017, JPhCS, 840, 012032
Górski, K. M., Hivon, E., Banday, A. J., et al. 2005, ApJ, 622, 759
Gschwend, J., Rossel, A. C., Ogando, R. L. C., et al. 2018, A&C, 25, 58
Hartley, W. G., Almaini, O., Mortlock, A., et al. 2013, MNRAS, 431, 3045
Holz, D. E., & Hughes, S. A. 2005, ApJ, 629, 15
Huchra, J. P., Macri, L. M., Masters, K. L., et al. 2012, ApJS, 199, 26
Ilbert, O., Arnouts, S., McCracken, H. J., et al. 2006, A&A, 457, 841
Jones, D. H., Read, M. A., Saunders, W., et al. 2009, MNRAS, 399, 683
Leistedt, B., Peiris, H. V., Elsner, F., et al. 2016, ApJS, 226, 24
LIGO Scientific CollaborationVirgo Collaboration, GBM, F., et al. 2017, arXiv:1710.05833
LIGO Scientific CollaborationVirgo Collaboration 2017, GCN, 21934, 1
Lima, M., Cunha, C. E., Oyaizu, H., et al. 2008, MNRAS, 390, 118
Lipunov, V. M., Gorbovskoy, E., Kornilov, V. G., et al. 2017, ApJL, 850, L1
LSST Dark Energy Science Collaboration 2012, arXiv:1211.0310
Macaulay, E., Nichol, R. C., Bacon, D., et al. 2019, MNRAS, 486, 2184
MacLeod, C. L., & Hogan, C. J. 2008, PhRvD, 77, 043512
Mandel, I., Farr, W. M., & Gair, J. R. 2019, MNRAS, 486, 1086
Mapelli, M., Giacobbo, N., Toffano, M., et al. 2018, MNRAS, 481, 5324
Morganson, E., Gruendl, R. A., Menanteau, F., et al. 2018, PASP, 130, 074501
Mortlock, D. J., Feeney, S. M., Peiris, H. V., Williamson, A. R., & Nissanke, S. M. 2018, arXiv:1811.11723
Mörtsell, E., & Dhawan, S. 2018, JCAP, 9, 025
Nair, R., Bose, S., & Deep Saini, T. 2018, PhRvD, 98, 023502
Nishizawa, A. 2017, PhRvD, 96, 101303
Nissanke, S., Holz, D. E., Dalal, N., et al. 2013, arXiv:1307.2638
Nissanke, S., Holz, D. E., Hughes, S. A., Dalal, N., & Sievers, J. L. 2010, ApJ, 725, 496
Palmese, A., Annis, J., Burgad, J., et al. 2019, MNRAS, submitted
Palmese, A., Hartley, W., Tarsitano, F., et al. 2017, ApJL, 849, L34
Palmese, A., Lahav, O., Banerji, M., et al. 2016, MNRAS, 463, 1486
Planck Collaboration, Aghanim, N., Akrami, Y., et al. 2018, arXiv:1807.06209

Pozzetti, L., Bolzonella, M., Zucca, E., et al. 2010, A&A, 523, A13
Riess, A. G., Casertano, S., Yuan, W., et al. 2018, ApJ, 861, 126
Riess, A. G., Macri, L. M., Hoffmann, S. L., et al. 2016, ApJ, 826, 56
Sadeh, I., Abdalla, F. B., & Lahav, O. 2016, PASP, 128, 104502
Schutz, B. F. 1986, Natur, 323, 310
Shectman, S. A., Landy, S. D., Oemler, A., et al. 1996, ApJ, 470, 172
Singer, L. P., Chen, H.-Y., Holz, D. E., et al. 2016, ApJS, 226, 10
Soares-Santos, M., Holz, D. E., Annis, J., et al. 2017, arXiv:1710.05459
Soares-Santos, M., Kessler, R., Berger, E., et al. 2016, ApJL, 823, L33
Tanvir, N. R., Levan, A. J., González-Fernández, C., et al. 2017, ApJL, 848, L27
The Dark Energy Survey Collaboration 2005, arXiv:astro-ph/0510346
Valenti, S., Sand, D. J., Yang, S., et al. 2017, ApJL, 848, L24
Vitale, S., & Chen, H.-Y. 2018, PhRvL, 121, 021303
Wechsler, R. H., & Tinker, J. L. 2018, ARA&A, 56, 435
Weigel, A. K., Schawinski, K., & Bruderer, C. 2016, MNRAS, 459, 2150